

# Therapeutic Radionuclides: Production, Physical Characteristics, and Applications

Suresh C. Srivastava and Leonard F. Mausner

## Contents

<b>1</b>	<b>Introduction</b> .....	12
1.1	Radionuclides.....	12
1.2	Therapeutic Particle Emissions.....	13
1.3	Selection Criteria for Therapeutic Radionuclides.....	13
1.4	Theragnostic Radionuclides.....	17
1.5	Availability Issues.....	18
<b>2</b>	<b>Radionuclide Production</b> .....	19
2.1	Nuclear Reactions.....	19
2.2	Production Equation.....	22
2.3	Sources of Nuclear Particles.....	22
<b>3</b>	<b>Reactor Production Using Neutrons</b> .....	25
<b>4</b>	<b>Accelerator Production Using Charged Particles</b> .....	26
<b>5</b>	<b>Targetry</b> .....	27
5.1	Physical and Chemical Form.....	27
5.2	Thermal Properties.....	27
5.3	Chemical Stability.....	27
5.4	Purity.....	27
5.5	Encapsulation.....	27
5.6	Availability.....	28
5.7	Target Transport Systems.....	28
<b>6</b>	<b>Radiochemical Processing and Purification</b> .....	28
6.1	Solvent Extraction.....	28
6.2	Chromatography.....	28
6.3	Distillation.....	29
6.4	Precipitation.....	29
6.5	Shielded Facilities.....	29
6.6	Current Requirements and Challenges.....	29
<b>7</b>	<b>Production of Selected Therapeutic Radionuclides</b> .....	30
7.1	Beta Emitters.....	31
7.2	Alpha, Auger, and Conversion Electron Emitters.....	36
<b>8</b>	<b>Conclusion</b> .....	45
	<b>References</b> .....	46

## Abstract

This chapter will focus primarily on the selection criteria, production, and the nuclear, physical, and chemical properties of therapeutic radionuclides, including those that are currently being used, or studied and evaluated, and those that warrant future investigations. Various scientific and practical issues related to the production and availability of these radionuclides will also be addressed. It is expected that this chapter will form the basis for the other chapters in this volume that will in much greater detail deal with radiopharmaceuticals based on a number of these therapeutic radionuclides and their present and potential usefulness in the clinical setting for treating cancer and other disorders. We are also reintroducing and reinforcing our recently proposed paradigm that involves specific individual “dual-purpose” radionuclides or radionuclide pairs with emissions suitable for both imaging and therapy, and which when molecularly (selectively) targeted using appropriate carriers, would allow pre-therapy low-dose imaging *plus* higher dose therapy in the same patient. We have made an attempt to sort out and organize a number of such *theragnostic* radionuclides and radionuclide pairs that may thus potentially bring us closer to the age-long dream of *personalized* medicine for performing *tailored* low-dose molecular imaging (SPECT/CT or PET/CT) to provide the necessary pre-therapy information on bio-distribution, dosimetry, the limiting or critical organ or tissue, and the maximum tolerated dose (MTD), etc., followed by performing higher dose targeted molecular therapy in the same patient with the same radiopharmaceutical. Beginning in the 1980s, our work at Brookhaven National Laboratory (BNL) with such a “dual-purpose” radionuclide, tin-117m, convinced us that it is arguably one of the most promising theragnostic radionuclides and we have continued to concentrate on this effort. Our results with this radionuclide are therefore covered in somewhat greater detail in this chapter. A major problem

S. C. Srivastava (✉) · L. F. Mausner  
Collider-Accelerator Department, Building 801,  
Brookhaven National Laboratory, Upton,  
NY 11973-5000, USA  
e-mail: suresh@bnl.gov

that continues to be addressed but remains yet to be fully resolved is the lack of availability, in sufficient quantities and at reasonable cost, of a majority of the best candidate radionuclides in a no-carrier-added (NCA) form. A brief description is provided of the recently developed new or modified methods at BNL for the production of five theragnostic radionuclide/radionuclide pair items, as well as some other therapeutic radionuclides which have become commercially available, whose nuclear, physical, and chemical characteristics seem to show promise for therapeutic oncology and for treating other disorders that respond to radionuclide therapy.

---

## 1 Introduction

Nuclear medicine has experienced an exponential resurgence of interest in radiotherapeutic procedures. Using unsealed sources for radionuclide therapy is not a new concept; it has been around for over five decades starting with the development of among others the treatment of thyroid disorders with radioiodine. However, recent advances in molecular biology have led to a better understanding of cancer and other disease states, and parallel research has shown promise for biological vehicles such as monoclonal antibodies, specific proteins and peptides, and a variety of other intelligently designed molecules, to serve as specific carriers to deliver cell killing radiation into tumors in a highly localized fashion. These developments have led to a renewed interest in the exciting possibility of treating human malignancies with the systemic administration of radionuclides. A number of other relatively new modalities, such as the treatment of metastatic bone pain, radiation synovectomy, bone marrow ablation, and others, have given additional impetus to the need for research on therapeutic radionuclides tailored for specific applications. A major advantage of radionuclides is that they emit radiation of different radiobiological effectiveness and range of action. This offers the possibility of choosing a nuclide the physical and nuclear characteristics of which are matched with a particular tumor type, or the disease under treatment.

As the title implies, this chapter will focus primarily on the selection criteria, production, and the nuclear, physical, and chemical properties of therapeutic radionuclides, including those that are currently being used, or studied and evaluated, and those that warrant future investigations. Various scientific and practical issues related to the production and availability of these radionuclides will also be addressed. It is expected that this chapter will form the basis for the other chapters in this volume that will in much greater detail deal with radiopharmaceuticals based on a number of these therapeutic radionuclides and their present and potential usefulness in the clinical setting for treating

cancer and other disorders. In addition, certain dual-purpose (“*theragnostic*”) radionuclides that seem to offer the exciting potential of pre-therapy low-dose imaging followed by higher dose treatment in the same patient, thus possibly bringing us a major step closer to personalized medicine, will be discussed. We are reintroducing and reinforcing this relatively novel paradigm that involves specific individual *theragnostic* radionuclides or radionuclide pairs with emissions suitable for both imaging and therapy, and which when molecularly (selectively) targeted using appropriate carriers, would allow pre-therapy low-dose imaging *plus* higher dose therapy in the same patient. We have made an attempt to sort out and organize a number of such *theragnostic* radionuclides and radionuclide pairs that may thus potentially bring us a major step closer to the age-long dream of *personalized* medicine for performing *tailored* low-dose molecular imaging (SPECT/CT or PET/CT) to provide the necessary pre-therapy information on biodistribution, dosimetry, the limiting or critical organ or tissue, and the maximum tolerated dose (MTD), etc., followed by performing higher dose targeted molecular therapy in the same patient with the same radiopharmaceutical. Beginning in the 1980s, our work at Brookhaven National Laboratory (BNL) with such a “dual-purpose” radionuclide, tin-117m, convinced us that it is arguably one of the most promising theragnostic radionuclides and we have continued to concentrate on this effort. Our results with this radionuclide are therefore covered in somewhat greater detail in this chapter. A major problem that continues to be addressed but remains yet to be fully resolved is the lack of availability, in sufficient quantities and at reasonable cost, of a majority of the best candidate radionuclides in a no-carrier-added (NCA) form. A brief description is provided of the recently developed new or modified methods at BNL for the production of five theragnostic radionuclide/radionuclide pair items, as well as some other therapeutic radionuclides which have recently become commercially available and whose nuclear, physical, and chemical characteristics seem to show promise for therapeutic oncology and for treating other disorders that respond to radionuclide therapy.

### 1.1 Radionuclides

Each nuclear species (a nuclide) is characterized by the constituents of its nucleus, its atomic number  $Z$  (number of protons), and its number of neutrons. Species with the same atomic number and differing mass numbers are called isotopes. Isotopes of an element differ only in the number of neutrons—the electronic structure is the same thus assuring identical chemical and biochemical properties and behavior. Although the terms isotope and nuclide are often used interchangeably, nuclide is the more general term. Nuclides

may be stable, that is, they do not show any detectable spontaneous change. Other nuclides are unstable, that is, they transform by radioactive decay, during which process they emit photons (suitable for imaging) and/or particulate radiation that may have the therapeutic value. There are now over 2,300 known unstable nuclides, and 280 are stable or having half-lives of greater than  $10^{24}$  years and less than  $10^{32}$  years (the half-life of the proton or the age of the universe).

Most radioactive nuclides (radionuclides) are artificially produced by transforming a stable nuclide into an unstable state by bombardment with nuclear particles mainly neutrons, protons, deuterons, alphas, gammas, or some other nuclear particles. The source of these particles may be a radionuclide, a nuclear reactor, or a particle accelerator (Van de Graaf, cyclotron, linac, etc.). The great variety of radionuclides created has given rise to many applications in physics, biology, and of course, in clinical nuclear medicine for diagnostic imaging as well as for therapeutic applications. The biggest area is “Nuclear Oncology”, which as the name implies, deals with the diagnosis (nuclear/molecular imaging) and/or the treatment/management of cancer patients. The subject of this chapter is the production and physical characteristics of those radionuclides created by irradiation either in a nuclear reactor or in an accelerator for use in therapeutic oncology and for other treatments that respond to radionuclide therapy.

## 1.2 Therapeutic Particle Emissions

Therapeutic particle emissions consist of Auger electrons, alpha emission, beta particles, and conversion electrons. Except for the beta particles, all of these are classified as high-linear energy transfer (LET) electron emitters. Conversion electrons in addition are generally monoenergetic and they have a discrete range in tissue, as opposed to beta electrons that have a range of energies, and thus a maximum and an average energy value. Auger electrons are very effective in cell kill but proximity to cellular DNA is often a necessary requirement. Alpha emitters are generally effective over several cell diameters ( $\sim 4$  to  $10$ ), whereas conversion electron emitters (depending upon energy) are effective over 0–50 cell diameters. This is depicted schematically in Fig. 1, which uses tin-117m as an example of conversion electron emitters (Srivastava 2012a).

In general, all high-LET emitters are much more effective for small lesions and for micrometastatic disease. For example, with a decrease in tumor size from 1 to 0.2 mm, the alpha emitter At-211 (energy transfer  $\sim 80$  keV/mm) is 9–33 times more effective than the low LET ( $\sim 1$  keV/mm) Y-90. At the cell surface, At-211 is 1,200 times more effective than the high-energy beta emitter Y-90 (Srivastava

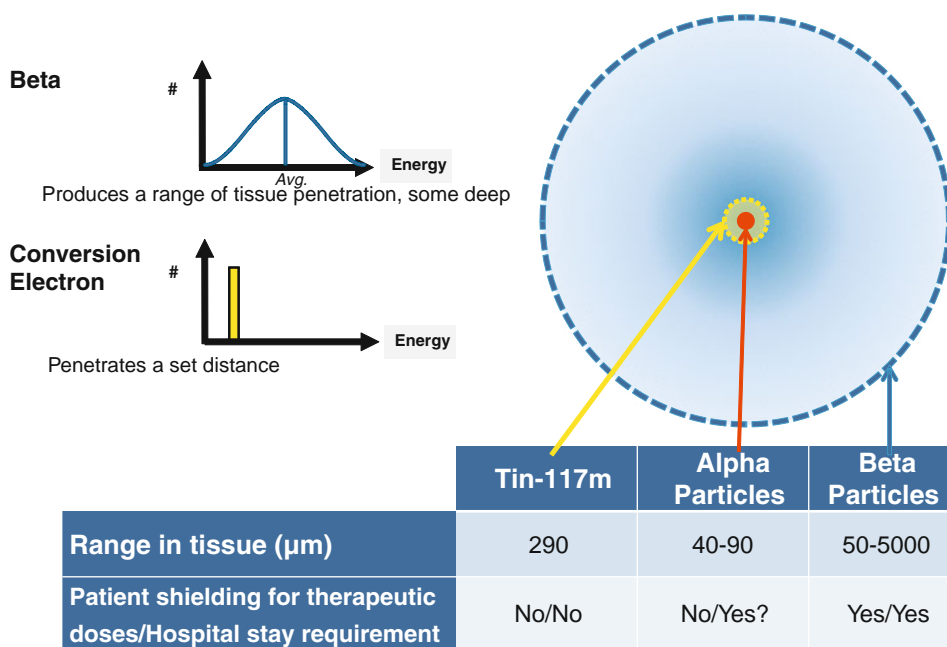
1996a, b, c). Because of their shorter range, and since there is none or insignificant crossfire, high-LET emitters may be less effective for large tumor masses and macrometastatic disease, even though the distribution within the lesion may be homogeneous. High-LET radiopharmaceuticals require a higher degree of selectivity of localization and this requires better and more specific targeting mechanisms. Ultimately, the selection of an appropriate particle emitter depends upon the nature, the extent, and stage of disease. Conversion electrons by definition are associated with internal conversion which is an isoenergetic radiationless transition between two electronic states. Certain low-energy conversion electron emitters, for example tin-117m, offer an almost ideal combination of properties (Srivastava 2012). Tin-117m emits an imageable gamma photon in good abundance and short-range conversion electrons with a high linear energy transfer, and a high  $S$  value, which results in high quality therapeutic radiation. These properties can translate into a very high localized dose to diseased tissue with minimal toxicity to normal organs or non-target tissues, as long as the targeting is very specific. Commonly used beta emitters in comparison have much lower linear energy transfer and the emitted electrons resemble a plume that travels over a longer distance which translates into less intense localized therapeutic effect. However, they are often better suited for treating bigger lesions or macro-metastatic disease due to the cross-fire effect (Srivastava 2006).

## 1.3 Selection Criteria for Therapeutic Radionuclides

The selection criteria must be based on the physical data about the radionuclide, its production and chemistry, and biological variables governing its use. The important physical variables to consider include the radionuclide half-life, the type, energy, and branching ratio of particulate radiation and the gamma-ray energies and abundances. It is important to match the physical half-life with the in vivo pharmacokinetics of the carrier molecule used for targeting. If the half-life is too short, most decay will have occurred before the radiolabeled targeting molecule (radioconjugate) has reached the maximum tumor-to-background ratio.

Conversely, considerations of tumor radiobiology and low radioconjugate-specific activity concentration may also limit the use of long-lived radionuclides. For equal radioactivity concentrations in the target, radionuclides with long half-lives will produce a lower absorbed dose rate than those with short lifetimes. If the maximum absorbed dose rate from beta particles is much lower than that typical in brachytherapy (40–60 cGy/h), cell kill per cGy will be decreased (Fowler 1991; Dale 1985). The theoretical low

**Fig. 1** A schematic comparison of energy types for therapeutic radionuclides (Srivastava 2012)



specific activity of longer lived radionuclides would thus require a large mass of radionuclide, ligand, and the carrier molecule to achieve adequate dose rate. This can make the use of long-lived radiolabels less desirable. However, if a two- or three-stage therapy approach is utilized (Britton et al. 1991), it becomes useful to consider the use of long-lived beta emitters, e.g., P-32 and others. To some extent, the problem of low target dose rate may be counteracted by a number of factors including high non-penetrating equilibrium dose constant, high target to nontarget ratio, high carrier labeling efficiency, and the ability to administer a large carrier molecule mass (tumor saturation effect).

The type of particulate emission also must be considered. The potent lethality of Auger and low-energy conversion electrons has been demonstrated (Bradley et al. 1975; Chan et al. 1976; Kassis et al. 1982; Adelstein and Kassis 1987; Feinendegen 1975). As mentioned earlier (Srivastava 1996a, b, c, 2012), this effect can best be realized with intranuclear localization of the radionuclide, which does not generally occur with many radioconjugates, in particular peptides and monoclonal antibodies (Srivastava 1988). Of course,  $\alpha$  particles have a high LET effective in cell killing and a range of several cell diameters, 40–80  $\mu\text{m}$ . The short ranges will accentuate inhomogeneous absorbed dose particularly when the radioconjugate deposition is inhomogeneous. Beta particles are less densely ionizing and have a range longer than  $\alpha$ 's so that the distribution requirements are less restrictive for treatment (e.g., radioimmunotherapy, RIT) of bulky disease. On the other hand, for disseminated metastatic disease or micrometastases, the absorbed fraction for higher energy beta particles (range > tumor size) is decreased, leading to a less favorable tumor absorbed dose.

The gamma-ray energies and abundances are also important physical properties, because the presence of gamma rays offers the possibility of external imaging for biodistribution and dosimetry. These physical properties alone can be used to calculate radiation absorbed dose at the cellular level. This approach has been used by Jungerman et al. (Jungerman et al. 1984) to estimate delivered doses for RIT. An approach which explicitly includes biodistribution and kinetic data by using an idealized time-dependent averaged target-to-nontarget uptake ratio is that of Wessels and Rogus (Wessels and Rogus 1984). Although the quantitative dose ratios are highly dependent on the input biodistribution data, a comparison of the relative effectiveness of the radiolabels was demonstrated. This relative efficacy was approximately constant for reasonable variation of model parameters in accordance with observed biological data. A similar approach was also used by Yorke et al. (Yorke et al. 1991). Also, Humm (Humm 1986) has considered the effect on monoclonal antibody (MAb) dosimetry of varying tumor size and of cold regions. These papers underscore the importance for therapy of a high ratio of non-penetrating to penetrating ( $\gamma$ ) radiations. The complex relationship between tumor curability with different radionuclides and tumor size has been reviewed by Wheldon and O'Donoghue (Wheldon and O'Donoghue 1990).

The main chemical variables to be considered in choosing a radionuclide for therapy with carrier molecules, in particular MABs and other proteins, and peptides, are the radionuclide-specific activity achievable, metal-ion contamination, the number of labels per MAB molecule obtainable without loss of immunological activity, and the stability of the radionuclide-protein attachment. The

specific activity, or amount of activity per mass of the element in question (MBq/mg), depends primarily on the method of production. Simple neutron absorption reactions (e.g.,  $n, \gamma$ ) generally give low specific activity since the radionuclide cannot be chemically separated from a target of the same element. Accelerator-based proton, deuteron, or alpha-induced reactions are intrinsically no-carrier-added (NCA) methods that do allow chemical separation of product from the target. This can also be achieved at reactors by neutron absorption reactions leading to an intermediate product with beta decay to the desired final product, or by fast neutron reactions such as  $(n, p)$ . The achievable specific activity of these NCA methods then largely depends on the impurity levels of the product element in the target or in various reagents used in processing. An often overlooked source of carrier is due to the direct production of stable isotopes of the product element. Although this effect is often negligible compared to carrier introduced with the target, it can become significant with very pure targets and high bombarding energies. With increasing energy, the typical peaks in nuclear excitation functions broaden, usually reaching a plateau at approximately 150–200 MeV, and reaction cross sections for neighboring isotopes become comparable over large energy ranges. Some of these issues have been reviewed for therapeutic radionuclides (Volkert et al. 1991).

The presence of metal ions other than the product is a concern as they can compete for binding sites on bioconjugates. It is largely controlled by the selectivity of the chemical separation scheme, but this process is not perfect. For example, a normally adequate separation factor of  $10^{-7}$  on a 10 g target still leaves 1  $\mu\text{g}$  of target in the product which may be of concern when labeling at low protein concentrations. Indeed, measurement of these stable species at low concentration in radioactive solutions is often a very difficult practical problem. Although various analytical procedures exist for detecting ions at less than part per million levels, for example atomic absorption, emission spectroscopy, mass spectroscopy, and X-ray fluorescence, etc., these techniques often take time, utilize expensive instrumentation, and may require a large fraction of the final product solution for the measurement. Generally, the sooner the radionuclide is used the better, because its specific activity is highest, and this need competes with the desire to measure the specific activity and impurity levels. Also, it is typical for many research groups that the expensive analytical apparatus is not wholly owned. Instead, access is through a shared use facility whose operators are very reluctant to introduce radioactive material into their equipment. Thus the fastest, albeit indirect method, of determining carrier levels may simply be by titration with the bioconjugate chelate during labeling.

The convenience, efficiency, and gentleness of various radiolabeling procedures as well as the stability of the radionuclide attachment to the antibody are all very important factors which are being actively investigated by many groups. They will not be considered further here as these topics are beyond the scope of this chapter and will be discussed elsewhere in this volume, and have also been reviewed previously (Fritzberg et al. 1988; Hnatowich 1990; Gansow 1991; Srivastava and Mease 1991). While recognizing the difficulties in designing new conjugation (labeling) schemes, at this point it is simply assumed that adequate radiolabeling techniques either exist or will become available for use with radionuclides to be discussed (Gansow 1991; Srivastava and Mease 1991). However, another practical aspect to be considered is that of radionuclide production—the routine availability, at reasonable cost, of quantities of radioactivity suitable for therapy. At present, very few therapeutic radionuclides truly meet all of these production criteria. However, this situation is changing for several other attractive radionuclides to be discussed in this chapter.

These physical and chemical factors must then be viewed in light of available biological information. For example, in the case of MAbs, there is substantial variation in uptake, macro- and micro-distribution, kinetics, and processing (metabolism/catabolism) depending on the particular antibody, antibody dose, the variability of antigenic expression in the tumor, its size and stage, etc. Limitations due to normal tissue radiotoxicity are not entirely the function of radionuclide emissions but are largely governed by the pharmacokinetics of the antibody. For many of the MAbs and MAb fragments currently being investigated for immunotherapy some generalities do emerge. It is generally believed that one-half to 3 days is usually required to reach maximum tumor uptake (DeNardo et al. 1982, 1988; Larson et al. 1988; Scheinberg and Strand 1983) although optimum contrast with whole MAbs may take longer. Despite the presence of numerous antigen sites on cancer cells, evidence from tumor implanted microthermoluminescent dosimeter probes (Wessels et al. 1985; Griffith et al. 1988) and autoradiography (Buechegger et al. 1988) indicates a non-uniform cellular distribution of the MAb in most cases. This may be due to cell-type heterogeneity (Buick et al. 1983), heterogeneity of antigenic expression (Fabre and Daar 1983), poor delivery, and spatial inaccessibility. These factors considerably reduce the attractiveness of short-ranged alpha-emitting radionuclides for radioimmunotherapy. A role for alpha emitters may be feasible in specific cases such as for micrometastases or intracavitary administration for some types of cancers, such as peritoneal injection for ovarian carcinoma (Bigler and Zanzanico 1988; Wilbur 1990). The longer range of beta particles can still permit uniform tumor irradiation despite a marked heterogeneity of

**Table 1** Present and future therapeutic radionuclides

Nuclide	T <sub>1/2</sub>	Particle emission <sup>a</sup>	E <sub>avg</sub> , keV <sup>b</sup> (% per decay)	Principal gamma component E, keV(%)
P-32 <sup>c</sup>	14.3 days	$\beta^-$	695	–
Sc-47	3.3 days	$\beta^-$	162	159 (68)
Cu-67	2.6 days	$\beta^-$	141	185 (49)
Ga-67	3.3 days	Aug	0.04–9.54 (572)	93 (37)
As-77	1.6 days	$\beta^-$	228	239 (1.6)
Sr-89 <sup>c</sup>	50.5 days	$\beta^-$	583	–
Y-90 <sup>c</sup>	2.7 days	$\beta^-$	935	–
Rh-105	1.5 days	$\beta^-$	190	319 (19)
Pd-109	0.6 days	$\beta^-$	360	88 (4)
Ag-111	7.5 days	$\beta^-$	350	342 (7)
In-111	2.8 days	Aug	0.5–25 (308)	171 (90); 245 (94)
Sn-117m	14.0 days	C.E.	127–152 <sup>d</sup>	159 (86)
I-123	13.2 h	Aug	0.7–30 (289)	159 (83)
I-125	60.1 days	Aug	0.7–30 (479)	36 (7)
I-131	8.0 days	$\beta^-$	181	364 (81)
Sm-153	1.9 days	$\beta^-$	225	103 (28)
Gd-159	0.8 days	$\beta^-$	311	363 (8)
Dy-165	2.33 h	$\beta^-$	438	95 (4)
Ho-166	1.1 days	$\beta^-$	666	80 (6)
Er-169 <sup>c</sup>	9.3 days	$\beta^-$	111	–
Lu-177	6.7 days	$\beta^-$	140	208 (11)
Re-186	3.7 days	$\beta^-$	329	137 (10)
Re-188	0.7 days	$\beta^-$	795	155 (15)
Ir-194	0.8 days	$\beta^-$	808	328 (13)
Hg-195 m	1.7 days	C.E.	13–259 (180)	262 (32)
		Aug	2.5–9.6 (409)	
Pt-195 m	4.0 days	C.E.	17–130 (276)	99 (11)
		Aug	2.4–63 (466)	
Au-198	2.7 days	$\beta^-$	311	412 (95)
Au-199	3.1 days	$\beta^-$	143	158 (37)
Tl-201	3.0 days	Aug	2.7–77 (253)	167 (11)
At-211	7.2 h	$\alpha$	5868 (41)	79 (21.3)
Bi-212	61 min	$\alpha$	6051 (25)	727 (7)
		$\alpha$	2246 (max)	
Bi-213	46 min	$\alpha$	1390 (max)	440 (26)
		$\alpha$	5870	
Ra-223	11.43 days	$\alpha$	5979	several gammas
				12–351
				81–95 (52)
Ac-225	10.0 days	$\alpha$	5915 <sup>e</sup>	99(93)
Fm-255	0.8 days	$\alpha$	7030 (93)	109 (24.6)

<sup>a</sup>  $\beta^-$  beta electrons; C.E. conversion electrons;  $\alpha$  alpha particles; Aug Auger electrons

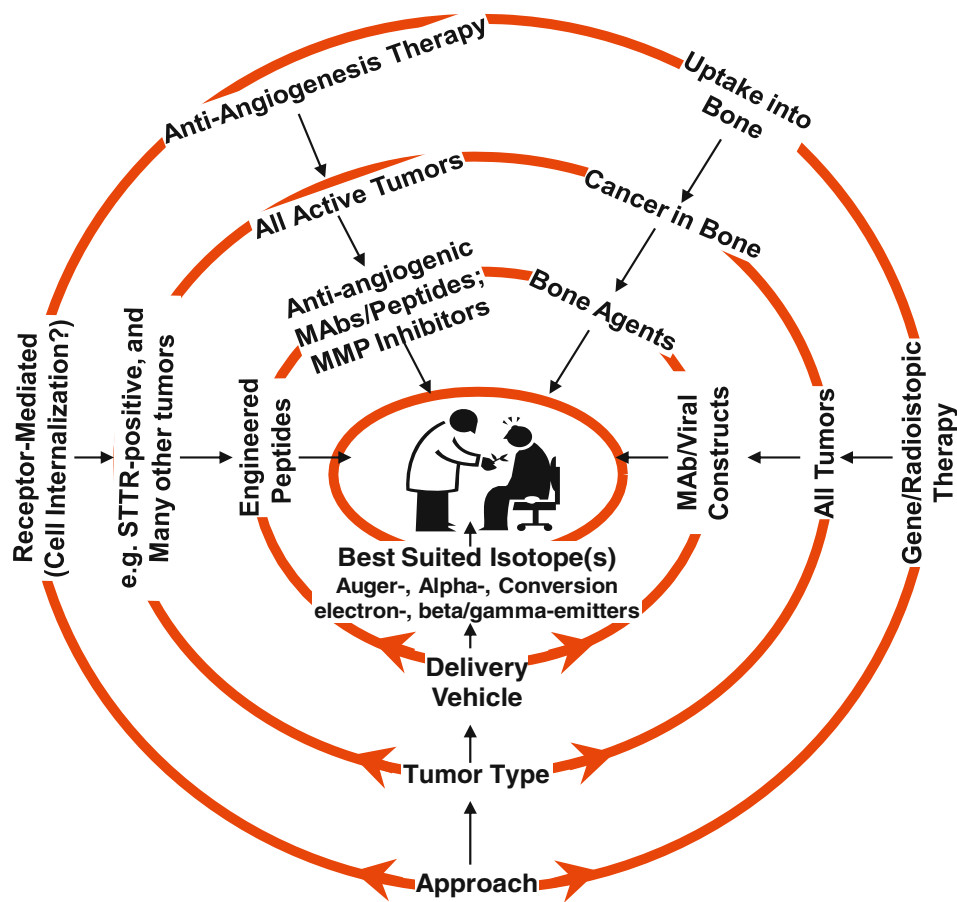
<sup>b</sup> Weighted average; total (%) per decay in parentheses

<sup>c</sup> No gamma emission

<sup>d</sup> Discrete energies

<sup>e</sup> Multiple decays to stable Bi-209; total energy ~ 28 MeV

**Fig. 2** Schematic representation of the central role of radionuclides for certain promising approaches for therapy of cancer



distribution of radioactivity within the tumor. It appears desirable to deliver ionizing radiation with a range of one to several millimeters in tissue, as from intermediate to high-energy beta particles.

A list of current as well as future therapeutic radionuclides, chosen arbitrarily on the basis of particle emission and a few other parameters, is presented in Table 1. The nature of the delivery vehicle depends upon the mechanisms that could be used to selectively target lethal doses of the radionuclide to the diseased tissue. A few representative examples of the approaches for cancer therapy using suitable radionuclides are shown schematically in Fig. 2.

#### 1.4 Theragnostic Radionuclides

As mentioned in the text earlier, radionuclides have a major advantage in that they emit radiation of different radiobiological effectiveness and range of action, which offers the possibility of choosing a nuclide the physical and nuclear characteristics of which are matched with a particular tumor type, or the disease under treatment. Also, certain radionuclides or radionuclide pairs have emissions that allow pre-therapy information with low-dose imaging,

followed by higher dose therapy in the same patient (Srivastava 2009, 2010, 2011, 2012). Such dual-purpose theragnostic radionuclides, for example I-131, or the pair I-124/I-131 have been around and used for imaging followed by therapy, without consideration of the fact that the optimum radionuclide or the optimum radionuclide pair was not scientifically or methodically chosen with this requirement and/or with the particular disease in mind. Over two decades ago, when Y-90 began to be promoted for radioimmunotherapy and was undergoing rapid development, it was considered necessary to use In-111-MAb as a surrogate to carry out biodistribution and imaging studies in order to predict the dosimetry and toxicity prior to doing the therapy with Y-90-MAb, because of the lack of imageable photons in Y-90 emissions. After some very careful studies, the Julich group (Herzog et al. 1993) and our own group at Brookhaven (Srivastava 1988; Srivastava and Dadachova 2001) showed that at best, it was hazardous to do so because these were two different elements whose biochemistry had many similarities but also many striking dissimilarities as well. Interestingly, this practice still continues, because of the lack of an alternate solution (Traub-Weidinger et al. 2011). In such a situation, it would have been best to use the positron emitter Y-86, a congener of Y-90, and therefore

with the same chemical and biochemical properties, to carry out pre-therapy PET imaging, so that imaging predicts biodistribution and dosimetry in a reliable, individualized fashion, and thus also predicts which patients will respond to the radionuclide therapy with Y-90 and which will not. However, Y-86 until very recently has not been available at all or only in insufficient quantities for this purpose. This situation is now changing and in many cases, if the therapeutic isotope has no photon emission, suitable congeners for imaging are becoming more and more available.

It is noteworthy that a number of such radionuclides or radionuclide pairs do exist (Srivastava 2009, 2010, 2011, 2012) and it would make a lot of sense to direct their use for the development of “theragnostic radiopharmaceuticals”. It is important to stress that *ideally*, for theragnostic use, the molecularly targeted radiopharmaceutical should constitute the same dual-purpose radionuclide with both imaging and therapeutic emissions. In the *second best* situation, as mentioned above for the Y-90 situation, a radionuclide pair (imaging photon emitter, either gamma or positron, and a congener of the therapeutic particle emitter, with the same electronic structure) can be used as well. One caveat here, which is a fact of life, is that even though many theragnostic PET/therapy radionuclide pairs may have the same electronic structure, their production and processing methodologies may be significantly different leading to the fact that their chemistry and in vivo behavior may be different as well due to differences in chemical species, charge, specific activity, etc., and/or the amount of chemical and radionuclidic and chemical impurities, which cannot be totally removed. Another caveat that one has to deal with is the issue of half-life of the imaging PET congener which in most cases might be much shorter than the usually (desirable) longer half-life of the therapeutic congener. In most situations, the determination of longer term biodistribution and dosimetry would be crucial but this information would not be achievable using the shorter-lived PET congener for pre-therapy imaging.

The theragnostic radionuclides or radionuclide pairs would initially allow molecular imaging (SPECT/CT or PET/CT) to provide the required and useful pre-therapy information on biodistribution, dosimetry, the limiting or critical organ or tissue, and the maximum tolerated dose (MTD). If the imaging results then warrant it, it would be safe and appropriate to follow-up with dose ranging experiments to allow higher dose targeted molecular therapy with the greatest effectiveness. These factors are especially important in order to be able to do *tailored* imaging *plus* therapy (personalized medicine) in the same patient with the same radiopharmaceutical (Srivastava 2009, 2010, 2011, 2012).

The discussion in this chapter that follows deals both with single theragnostic radionuclides, as well as the PET/

therapy theragnostic radionuclide pairs. In addition, a few other promising therapeutic radionuclides that have been under investigation and have become available commercially in sufficient quantities for clinical trials are included. There are indeed a number of individual radionuclides that emit both imaging photons and therapeutic electrons and which would be potentially excellent choices for theragnostic applications (Table 2). Some of the most promising PET/Therapy radionuclide pairs are shown in Table 3. The lists included in both Tables 2 and 3 are not all-inclusive but consist of selected radionuclides and radionuclide pairs that are or could be made available in sufficient quantities to be of practical value, and which show the required combination of nuclear, physical, and chemical properties, and thus the greatest promise. Some other criteria for inclusion were arbitrarily set at a minimum of 20 % photon/positron emission for imaging, and a sufficiently abundant therapeutic particle emission consisting of medium ( $\beta^-$ ) to high LET electrons. It should be noted that there may be other suitable candidates from the class of alpha and Auger electron emitters (Srivastava 1996a, b, 2006, 2012; Kassiss et al. 1982; Adelstein and Kassiss 1987; Feinendegen 1975), but these have not been included in this theragnostic group of radionuclides (except Ac-225/Bi-213) since their availability is either limited or not enough pre-clinical and clinical experimental data have thus far been available.

## 1.5 Availability Issues

A major problem that remains yet to be completely resolved is the lack of availability of a number of the best candidate therapeutic radionuclides, in particular the theragnostic radionuclides or PET/SPECT radionuclide pairs, in sufficient quantities and/or in a no-carrier-added (NCA) form. Methods have already been studied and developed for the production of research quantities of certain theragnostic radionuclides and radionuclide pairs listed in Tables 2 and 3 in particular Cu-64 (Szelecsenyi et al. 1993), Y-86 (Srivastava 2009, 2010, 2011, 2012; Sadeghi et al. 2009; Medvedev et al. 2011), I-124 (Aslam et al. 2001), and Sc-44 (Huclier-Markai et al. 2011). Gallium-67, Y-90, In-111, I-123, Sm-153, Lu-177, and I-131 are routinely available from commercial sources. Close to sufficient quantities of Ge-68 (parent of Ga-68) are made available mainly from the Brookhaven Linac Isotope Producer (BLIP) at Brookhaven National Laboratory (BNL) (Meinken et al. 2005) and from the Isotope Production Facility (IPF) at Los Alamos National Laboratory (LANL).

A summary description relating to the development of new or modified methods for the production of selected promising theragnostic radionuclides (Sc-47, Cu-67, Y-86, Sn-117m, and Ac-225/Bi-213), as well as a number of other

**Table 2** Selected theraagnostic radionuclides

Radionuclide	T <sub>1/2</sub> (days)	Principal $\gamma$ energy for imaging, KeV(%)	Therapeutic particle(s) (avg. energy, KeV, % abundance)
Scandium-47	3.35	159 (68)	$\beta^-$ (162)
Copper-67	2.58	186 (40)	$\beta^-$ (141)
Gallium-67	3.26	93, 184, 296 (40, 24, 22)	15 Auger, 0.04–9.5 keV, 572 % 10 C.E, 82–291 keV, 30 %
Indium-111	2.80	171, 245 (91, 94)	6 Auger, 0.13–25.6 keV, 407 % 12 C.E, 144–245 keV, 21 %
Tin-117m	14.00	159 (86)	8 C.E. (141 keV avg., 114 %)
Iodine-123	13.3 h	159 (83)	12 Auger, 23–30.4 keV, 1371 % 7 C.E, 0.014–32 keV, 17 %
Iodine-131	8.0	365 (82)	$\beta^-$ (181)
Samarium-153	1.94	103 (30)	$\beta^-$ (280)
Astatine-211	7.2 h	79 (21)	$\alpha$ (5867, 42 %)
Bismuth-213	46 min	441 926)	$\beta^-$ (425); $\alpha$ (98 %, from Tl-209 daughter, 2 % from Bi-213)

**Table 3** Selected theraagnostic radionuclide pairs

Radionuclide pair imaging/therapeutic	T <sub>1/2</sub> (days)	Imaging positron, KeV (%)	Therapeutic particle(s) (avg. energy, KeV)
Scandium-44/Scandium-47	3.97/3.35	$\gamma \pm 511$ (99.9%)	$\beta^-$ (162)
Copper-64/Copper-67	0.53/2.6	$\gamma \pm 511$ (38%)	$\beta^-$ (141)
Gallium-68/Gallium-67	68 min/3.26	$\gamma \pm 511$ (176%)	15 Auger, 0.04–9.5 keV, 572 % 10 C.E., 82–291 keV, 30 %
Yttrium-86/Yttrium-90	0.61/2.7	$\gamma \pm 511$ (35%)	$\beta^-$ (935)
Iodine-124/Iodine-131	4.2/8.0	$\gamma \pm 511$ (38%)	$\beta^-$ (181)

therapeutic radionuclides that have recently become available in reasonable quantities and/or have undergone through various stages of clinical trials, is included in the following sections.

## 2 Radionuclide Production

Basically, radionuclides can be classified into two main groups, those that are neutron-rich and those that are neutron-deficient. Although this classification is not completely accurate, for the purposes of this chapter, it serves to separate the radionuclides which are usually made in a reactor from those that are made using a particle accelerator. Those that are neutron-rich are usually made in a nuclear reactor while those that are neutron-deficient (or in most cases, NCA) are produced by bombarding a suitable target with protons, deuterons, or helium particles.

Particle accelerators and especially cyclotrons have been very important in the preparation of radioisotopes during the 1930s until World War Two (WWII). The amount of radioactive material that could be produced in an accelerator was several times greater than the amount which could be produced using the alpha particles from naturally

occurring radioactive elements. After WWII, reactors began to be used to produce radioactive elements and the use of accelerators for this purpose became less common. However, as the techniques for using radiotracers became more sophisticated, it became clear that reactor produced radionuclides could not satisfy the growing demands and therefore, accelerators were considered preferable and needed to produce new radionuclides which could be used in additional new ways.

As mentioned earlier, among all the therapeutic (or imaging for that matter) radionuclides that have ever been produced, or those that continue to be investigated for production, only a very few have or will end up with the required combination of favorable nuclear, physical, and biological characteristics to become useful for routine clinical use.

### 2.1 Nuclear Reactions

Many processes can occur when nuclear particles strike a target. Generally, charged particles first collide with atomic electrons producing *ionization* and *excitation* of these atoms. Energy is transferred to these electrons thus

decreasing the energy of the incident charged particle. The electron energy is ultimately converted into heat. This process can be visualized as the particle plowing through a sea of electrons and dissipating its energy through friction. Neutrons carry no charge, and their interaction with electrons is negligible.

Although relatively infrequent compared to electron interactions, sometimes the incident particle comes close enough to the very small atomic nucleus to transfer some kinetic energy to the nucleus as a whole. The nucleus moves but has no internal excitation. This process is called *nuclear elastic scattering* and may be visualized as billiard balls colliding. The energy of nuclear motion also eventually dissipates as heat. If the collision involves a close approach of projectile to target nucleus, the particle will be affected by short-range nuclear forces as well as by the Coulomb forces. In this case the direction of the particle changes and it loses kinetic energy to the nucleus, which may become internally excited. Kinetic energy is not conserved in this process which is called *nuclear inelastic scattering*. The nucleus de-excites very quickly by the emission of one or more gamma rays.

Finally, a particle may be absorbed by the target nucleus that is then excited by the transfer of kinetic energy and the released binding energy of the incident particle. This incident particle is captured and a new heavier nucleus is formed, at least briefly. The highly excited intermediate nucleus can nearly instantaneously de-excite in several ways. It can emit electromagnetic radiation in the form of gamma rays. These gamma rays are called “prompt” to distinguish this mechanism from gamma emission following radioactive decay. If the incident particle is a neutron, this process is called radiative capture. If the nuclear excitation energy is concentrated on a few nucleons (i.e. neutrons and protons), either by direct collision with the incident particle or by statistical processes, nucleons can be ejected. If the total excitation energy of the intermediate state is greater than the binding energy of nucleons within the nucleus, nucleon emission is favored. If not, simple prompt gamma emission returns the new nucleus to a more stable state. This process of conversion of the original nucleus into a new one is a *nuclear reaction*, and the residual nucleus is the reaction product. This process in which the reaction product is radioactive is of major interest to nuclear medicine.

In the case of neutron bombardment (e.g., in a reactor), there is no Coulomb repulsion from the positively charged nucleus, and neutrons easily penetrate the nucleus. Actually, very low energy neutrons have very large reaction probabilities, and are thus particularly useful for radionuclide production. These neutrons are called “thermal neutrons”, because they have an energy distribution of that of ordinary gas molecules in thermal equilibrium at room temperature.

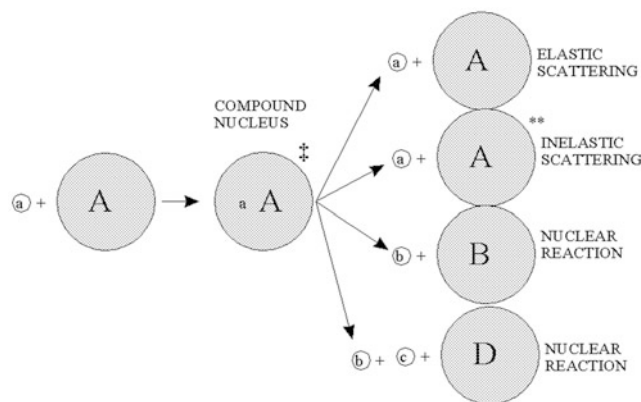
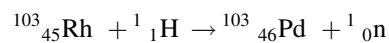


Fig. 3 The compound nucleus (Bohr 1936)

The most probable energy is 0.025 electron volts (eV). Neutrons with energies up to about several keV are often called “epithermal” or “resonance” neutrons, and higher energy neutrons are simply referred to as “fast neutrons”.

Nuclear reactions are written in equation form in analogy to chemical reactions, with the reactants on the left and the products on the right-hand side. For example, the reaction between Rh-103 and a proton to produce Pd-103 and an emitted neutron is written as:



More frequently a short-hand notation is used where the incident and emitted particles are written in parentheses or brackets between the initial and final nuclei. Atomic numbers are omitted. Thus, the above reaction is abbreviated  $^{103}\text{Rh}[\text{p}, \text{n}]^{103}\text{Pd}$ . Elementary particles and certain light nuclides have their own symbols, such as n, p, d, t,  $\alpha$ ,  $\gamma$ ,  $\beta$ , e,  $\pi$  representing the neutron, proton, deuteron ( $^2_1\text{H}$ ), triton ( $^3_1\text{H}$ ), alpha particle ( $^4_2\text{He}$ ), gamma ray, beta particle, electron, and pi meson, respectively.

A complete detailed theory of nuclear reactions in terms of basic nuclear forces is not yet available. Instead, approximate treatments based on models are used for understanding measurements and have proved useful for predictive purposes. An early model useful to radionuclide production reactions was the compound nucleus model, introduced by Niels Bohr in 1936 (Bohr 1936), depicted in Fig. 3. In this model, the incident particle is absorbed into the nucleus of the target materials and the energy is distributed throughout the compound nucleus. In essence, the nucleus comes to some form of equilibrium before decomposing with the emission of particles. These two steps are considered to be independent of one another. It does not matter how the compound nucleus got to the high energy state; the evaporation of the particles will be independent of the way in which it was formed.

The nuclear reaction cross-section represents the total probability that a compound nucleus will be formed and that it will decompose in a particular channel. There is a minimum energy below which a nuclear reaction will not occur except by tunneling effects. The incident particle energy must be sufficient to overcome the Coulomb barrier and to overcome a negative energy of the reaction. Particles with energies below this barrier have a very low probability of reacting. The energy required to induce a nuclear reaction increases as the  $Z$  of the target material increases. For many low  $Z$  materials it is possible to use a low energy accelerator, but for high  $Z$  materials, it is necessary to increase the particle energy (Deconninck 1978).

The various above phenomena lead to a disappointing fact in radionuclide production. It is not always possible to eliminate the radionuclidic impurities even with the highest isotopic enrichment and the widest energy selection, especially using chemical methodology in cases where the radionuclide impurities are isotopes with the same proton number and the electronic structure. An example of this is given in Fig. 4 for the production of iodine-123 with a minimum of I-124 impurity (Guillaume et al. 1975; Lambrecht and Wolf 1973; Qaim and Stocklin 1983). As can be seen from this figure, it is almost impossible to eliminate the I-124 impurity from the I-123 because the I-124 is being made at the same energy, and the chemical properties defined by the electronic structure are the same. All that can be done is to minimize the I-124 impurity by choosing an energy level where the production of I-124 is near a minimum. In this specific case, proton energy higher than  $\sim 20$  MeV will give a minimum of I-124 impurity. This kind of an exercise is encountered in just about all situations with the production of medical radionuclides.

Fission is a special mode of nuclear de-excitation in the region of high atomic numbers. In spontaneous fission, the mutual electrostatic repulsion between protons of a very heavy nucleus can overcome the Coulomb barrier and causes the separation of a heavy nucleus into two lighter positively charged fragments, usually of unequal mass. There are over 60 known nuclides, which can spontaneously fission. For particle-induced fission, the bombarding particle supplies enough energy to overcome the barrier. In particular, thermal neutron fission of U-235 has had great significance for society. The 200 MeV energy release per reaction and release of an excess of neutrons made possible the development of both the atomic bomb and the nuclear reactor. Over 75 useful radionuclides are produced in this manner and are called fission products. Many of these can be separated and purified for medical, industrial, and research applications. Of interest for nuclear medicine are the light fragments resulting from induced fission, especially the fission products Mo-99, I-131 and Xenon-133. The production of Mo-99 has been of paramount

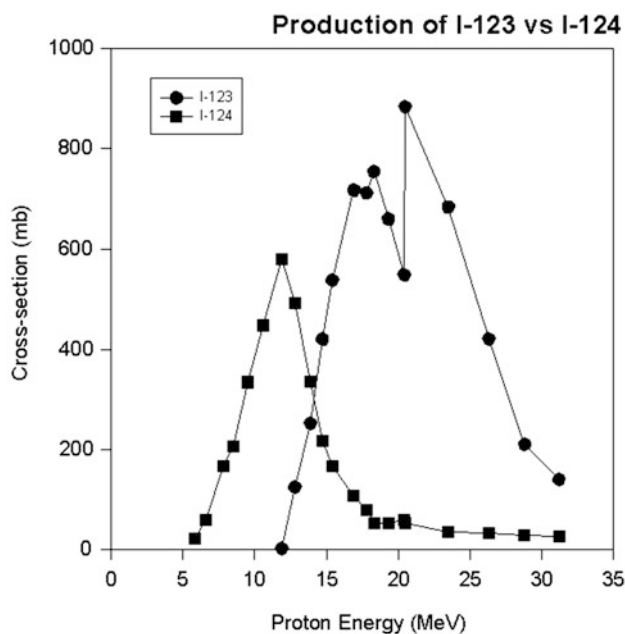


Fig. 4 Production of I-123 versus I-124 (Schlyer 2003)

importance to nuclear medicine. Molybdenum-99 is not directly used, but serves as the parent radionuclide for the daughter Tc-99m, now used diagnostically in over 85 % of all diagnostic imaging procedures in nuclear medicine worldwide (Richards et al. 1982). Iodine-131 is widely used to treat thyroid cancer and hyperactive thyroid conditions. Xenon-133 is used for studies of pulmonary ventilation and also for cerebral blood perfusion.

The compound nucleus model does not very well explain all the nuclear reaction processes. Some of these processes are characterized by direct interactions, where the incident particle collides with only one or a few nucleons in the target which are immediately ejected without sharing of energy throughout the nucleus. These “knock-on” reactions become increasingly important at bombarding energies of over about 40 MeV. Above about 100 MeV, collision with an individual nucleon is the most likely initial event, followed by its ejection from the nucleus. While passing through the nucleus this nucleon may in turn collide and eject another nucleon, leading to many successive nucleon–nucleon collisions. Some of these nucleons promptly escape while others undergo additional collisions in the nucleus. This “intranuclear cascade” is very rapid (duration  $\sim 10^{-22}$  s) and leaves the nucleus in a generally excited state from which it can lose more nucleons by evaporation. The sum of these interactions: knock-on; intranuclear cascade; and evaporation, is called the spallation process. Proton-induced spallation or breakup, has been used to produce a few radionuclides of interest to nuclear medicine, for example Xe-127, and Strontium-82. Although high-energy neutrons can also interact by a spallation process

(Mirzadeh et al. 1983) due to lack of high intensity fast neutron sources, radionuclide production by neutron-induced spallation is much more limited.

It is important that the total excitation energy of a compound nucleus formed by absorption of a thermal neutron is just above the energy to bind a neutron in the compound nucleus. Thus, the time before statistical fluctuation can concentrate enough energy on a single neutron to cause its ejection from the nucleus, would be quite long. As a result, de-excitation by  $\gamma$  emission is much more likely and the main reaction with thermal neutrons is the n,  $\gamma$  (neutron in, gamma out) process.

## 2.2 Production Equation

The production of a given radionuclide is proportional to the number of target nuclei  $N_t$ , number of incident particles  $\phi$  and the reaction cross-section  $\sigma$ , or  $R = N_t\phi\sigma$ . The product radionuclide itself undergoes radioactive decay,  $\lambda N_p$ . Thus, the net rate of change in the number of radioactive product nuclei,  $N_p$ , during irradiation is given by the rate of formation less the rate of decay, or

$$dN_p/dt = \phi\sigma N_t - \lambda N_p$$

Since  $N_t$  is so large as to remain essentially constant during irradiation, the solution to this differential equation is

$$\lambda N_p = N_t\phi\sigma (1 - e^{-\lambda t})$$

The activity of the product  $A_p$  at the end of bombardment (EOB) is  $\lambda N_p$ , and after substitution we obtain the radionuclide production equation,

$$A_p = N_t\phi\sigma (1 - e^{-\lambda t}),$$

where,  $A$  = activity in disintegrations per second, dps

$N_t$  = number of target atoms =  $W/M \times F \times \text{Avog}$

$W$  = sample weight in grams,

$M$  = atomic weight in grams/mole;

$F$  = isotopic abundance,  $\text{Avog}$  = Avogadro's number;  
 $6.023 \times 10^{23}$  atoms per mole]

$\phi$  = neutron flux in neutrons.cm<sup>-2</sup>.sec<sup>-1</sup>

$\sigma$  = cross-section in cm<sup>2</sup>

$\lambda$  = decay constant of product =  $\ln(2)/t_{1/2}$

$t$  = irradiation time

Note that at long irradiation times where  $\lambda t \gg 1$  (or  $t_{\text{irrad}} \gg t_{1/2}$  of the product) the factor  $(1 - e^{-\lambda t})$  approaches 1. This signifies that the rate of product formation and the rate of product decay are equal, and the reaction is said to be at "saturation". The term  $(1 - e^{-\lambda t})$  is also known as the saturation factor. Thus, longer irradiation time does not produce any more radioactivity. In practice, irradiations

longer than one half-life ("half saturation") are relatively inefficient since doubling the irradiation by another half-life only increases radioactivity from 50 to 75 % of saturation.

As an example of the use of the production equation, consider a 24-h irradiation of 1 mg of natural rhenium (37.4 % Re-185) in a thermal neutron flux of  $2 \times 10^{14}$  n cm<sup>-2</sup>.sec<sup>-1</sup> to make Re-186 ( $t_{1/2} = 3.718$  days). The tabulated cross-section is 112 barns (Mughabgab et al. 1984).

$$\begin{aligned} N_t &= (0.001 \text{ g}/186.21 \text{ gm per mole})(0.374 \text{ natural Re}) \\ &\quad (6.023 \times 10^{23} \text{ atoms/mole}) \\ &= 1.21 \times 10^{18} \text{ atoms} \end{aligned}$$

Then, the amount of Re-186 radioactivity produced is

$$\begin{aligned} A &= (1.21 \times 10^{18} \text{ atoms})(2 \times 10^{14} \text{ n.cm}^{-2}.\text{sec}^{-1}) \\ &\quad (112 \times 10^{-24} \text{ cm}^2) \times \\ &\quad [1 - \exp((-0.693/3.718 \times 24 \text{ h}) \times 24 \text{ h})] \\ &= 4.6 \times 10^9 \text{ atoms per second, or disintegrations per} \\ &\quad \text{second (dps)} \\ &= 124.3 \text{ mCi (1 mCi} = 3.7 \times 10^4 \text{ dps, or 37 MBq)}. \end{aligned}$$

Corrections to this result would be needed if the samples were large, or the irradiation was lengthened. For a massive target with a high cross-section, there is sufficient absorption of neutrons in outer layers so that the effective neutron flux in the interior of the target is reduced (self-shielding). This effect is difficult to calculate and is usually measured. Also, Re-186 itself can absorb a neutron and convert into Rhenium-187. This process is called product burn-up. While some conversion of Re-185 into Re-186 can also be induced by higher energy neutrons, most comes from the thermal neutrons considered here because thermal neutron fluxes are usually much larger than for higher energy neutrons.

The production equation can take one of two forms, depending upon whether the target is immersed in a bath of neutrons as in a nuclear reactor, or irradiated in a specific direction by a beam of particles from an accelerator. In the latter case, the target is usually larger than the diameter of the beam. The fraction of target irradiated is then important. An early detailed discussion of the equations governing the production of radionuclides, in particular with reactors, is presented in the article by Mirzadeh and Walsh (Mirzadeh and Walsh 1998).

## 2.3 Sources of Nuclear Particles

### 2.3.1 Nuclear Fission Reactor

Although there are neutron sources based on natural radioactivity and accelerators, the most generally useful source of neutrons for radionuclide production is the research nuclear reactor. A reactor consists of an amount of fissionable material, either U-235 (natural or enriched), Pu-239, or U-233, assembled so that a controlled, self-sustaining chain reaction of neutron-induced fissions is maintained. The fission of U-235 produces an average of 2.4

neutrons, two medium mass nuclei (fission products with average masses of 100 and 140 amu), and the release of approximately 200 MeV. Since fission is best induced with low energy neutrons, a moderator (usually water) is used to slow the emitted neutrons. Some neutrons are absorbed by the moderator and structural materials and some escape. A chain reaction can be sustained if at least one of the neutrons causes another U-235 to fission. This condition is expressed as the multiplicity factor  $k$  and a reactor is “critical” at  $k = 1$ . The U-235 is usually embedded in high melting zirconium hydride contained in metal tubes bundled together into fuel elements. The arrangement of fuel elements is called the core.

At steady state,  $k$  is kept at 1 but sometimes  $k$  must be made larger than 1. This allows the neutron flux and the power level to be varied, and compensates for fuel use (burn up), build-up of neutron-absorbing fission products, and the deliberate introduction of samples that absorb neutrons. The quantity  $(k-1)/k$  is called the reactivity, and reactors must be designed with excess reactivity. The reactivity and power level are determined by the position of control rods. These control rods are made of materials with large neutron capture cross-sections, such as boron, cadmium, and hafnium. Lowering control rods into the core reduces the number of neutrons available for fission. Some specially designed reactors control reactivity by moving the fuel elements themselves.

The most important fission product from the point of view of reactor operation is Xenon-135. It has a half-life of 9.1 h and a neutron capture cross-section of  $2.6 \times 10^6$  barns (b), the largest known. During steady-state reactor operation the build-up of Xe-135 is slow. However, upon shutdown the amount of Xe-135 initially increases rapidly due to grow-in from the decay of its parent, I-135 ( $t_{1/2} = 6.6$  h) and the decrease in  $(n, \gamma)$  reactions which destroy it. This Xe-135 “poisoning” peaks about 10 h after shutdown, and causes a large drop in reactivity (as much as 30 %). Since many reactors cannot overcome this much loss of reactivity, usually there is a period after shutdown during which the reactor cannot be restarted.

A nuclear reactor produces neutrons with a spectrum of energies up to about 20 MeV; the most probable energy of neutrons emitted in the fission process is 1.5 MeV. Neutrons are generally grouped into three categories, thermal neutrons ( $E_n < 0.4$  eV), epithermal neutrons (0.4 eV <  $E_n < 100$  keV), and fast neutrons ( $E_n > 100$  keV). The energy spectrum of the lowest energy neutrons approximates a Maxwellian distribution similar to that of ordinary gas molecules in equilibrium at room temperature; thus the name thermal neutrons. The peak of this distribution is at 0.025 eV. These neutrons are very efficient at producing nuclear reactions and are widely used for radionuclide production on a commercial basis. Epithermal (or

resonance) neutrons are formed when fast neutrons are partially slowed down by collisions with moderator. The fast neutrons arise from the fission process directly.

The use of reactors for power production is based on the large 200 MeV energy release per fission. Approximately 1 g/day of fissioned fuel produces 1 mw of reactor thermal power. Electrical output is only about one-third of the thermal power. Further discussion of reactor physics, safety and economics is beyond the scope of this chapter, but many references exist (Liverhaut 1960; Glasstone and Sesonske 1963; Cohen 1977).

Electrical power generation is generally incompatible with radionuclide production, so it is the research reactor which is of most interest here. These can take many different forms, but the vast majority of these have used enriched U-235 for fuel, with enrichment varying from 10 % to greater than 90 %. These typically thermalize the neutrons with moderators of water, D<sub>2</sub>O, or graphite. Power levels cover the range from 0.1 W (e.g., Aerojet General Corp. Teaching Reactor AGN-20) to 450 MW (Fast Flux Test Facility, Westinghouse Hanford Company, now shut down). Useable thermal neutron fluxes range from  $5 \times 10^6$  n cm<sup>-2</sup> s<sup>-1</sup> to  $\sim 2 \times 10^{15}$  n cm<sup>-2</sup> s<sup>-1</sup>. A summary of the maximum fluxes available at nine of the principal research reactors in the United States is given in Table 4.

Most research reactors have the entire core immersed in water (or D<sub>2</sub>O) and are often called swimming pool reactors. The 5–8 m of water functions not only as a moderator, but also for cooling and radiation shielding. Irradiation positions for samples typically exist between fuel rods (in-core locations) or in an annular region just inside a ring of low  $Z$  material with small neutron capture cross-section. This material (beryllium is often used) “reflects” neutrons back to the core and minimizes neutron losses. The reflector increases thermal neutron flux at irradiation stations and helps save fuel. The actual fluxes and neutron energies available for radionuclide production are a sensitive function of the detailed reactor design and vary with location within the reactor. A brief description of ORNL-HFIR and other major research reactors in the US has been provided in the article by Mausner and Mirzadeh (Mausner and Mirzadeh 2003).

### 2.3.2 Charged Particle Accelerators

In general, there are four major reasons that accelerator-produced radionuclides are used more widely than reactor-produced radionuclides: (1) The radionuclides produced in a reactor may have unfavorable decay characteristics (particle emission, half-life, gamma rays, etc.) for a particular application; (2) The radionuclide cannot usually be produced in a reactor with high specific activity; (3) Access to a reactor is limited; and, perhaps most importantly; (4) The radionuclide can be produced most efficiently and in a more

**Table 4** Principal research reactors in the United States

Reactor/Institution	Operating power (MW) (1–16 MeV)	Thermal	Neutron flux epithermal (0–0.25 eV)	Fast (0.25 eV–1 MeV)
Fast flux test facility <sup>a</sup> , Westinghouse Hanford Company	450	$5.2 \times 10^{14}$	$6.6 \times 10^{15}$	$3.7 \times 10^{14}$
Advanced test reactor, Idaho National Engineering Laboratory	250	$4.5 \times 10^{14}$	$6.7 \times 10^{14}$	$4.1 \times 10^{14}$
High flux isotope reactor, Oak Ridge National Laboratory	85	$5.3 \times 10^{15}$	$1.5 \times 10^{15}$	$5.8 \times 10^{14}$
High flux beam reactor <sup>a</sup> , Brookhaven National Laboratory	30	$4.2 \times 10^{14}$	$1.3 \times 10^{15}$	$1.5 \times 10^{14}$
Missouri University research reactor, University of Missouri	10	$4.2 \times 10^{14}$	$1.6 \times 10^{14}$	$7.0 \times 10^{14}$
Omega west reactor <sup>a</sup> , Los Alamos National Laboratory	8	$9.0 \times 10^{13}$	$5.0 \times 10^{12}$	—
Georgia Institute of Technology Research Reactor	5	$6.5 \times 10^{13}$	$1.7 \times 10^{12}$	$2.9 \times 10^{12}$
Massachusetts Institute of Technology, Reactor	5	$6.0 \times 10^{13}$	$3.0 \times 10^{13}$	$1 \times 10^{13}$
Oregon State University Triga Reactor	1	$1.0 \times 10^{13}$	$4.0 \times 10^{11}$	—

<sup>a</sup> recently shutdown

cost-effective manner in an accelerator. In addition, of late, the number of reactors available has become much fewer than the number of cyclotrons available to the scientific and industrial community.

There are a wide variety of nuclear reactions, which are involved in the accelerator production of radionuclides. These are very similar in principle with those discussed in Sect. 2.1 above. Nuclear reactions specific to accelerator production have been described and covered in detail by David Schlyer of BNL (Schlyer 2003).

The bombarding particles are usually protons, deuterons, or helium particles. The energies which are used range from a few MeV to hundreds of MeV (Gandarias-Cruz and Okamoto 1988). In these situations, one of the most useful models for nuclear reactions is also the compound nucleus model originally introduced by Bohr in 1936 (Bohr 1936), and described in Sect. 2.1 (Fig. 3).

One of the main concerns in targets, specifically in accelerator production, is the deposition of power in the material during irradiation (Schlyer 2003). If the power deposited exceeds the ability of the target to remove the heat, the target will eventually be destroyed or the target material will be melted, volatilized, or reduced in density to the point where the yield will be drastically reduced. In liquid targets the material may boil and thereby reduce the average density. In gaseous targets, the density of the gas is reduced in the beam strike area. All these effects are a result of the increased temperature in the beam strike area and this in turn is a result of the power deposited by the beam as it passes through matter. The power deposited in the material is the beam current in microamps ( $\mu\text{A}$ ) multiplied by the

energy loss in MeV and the result is the number of watts deposited.

$$\text{Power(watts)} = I(\text{microamps})\Delta E(\text{MeV})$$

The exact position of the heat deposition will depend on the  $dE/dx$  (stopping power) of the beam in the target material with most of the heat being deposited near the end of the particle range in the Bragg peak. A simple approximation for the stopping power is given by the relation:

$$\frac{dE}{dx} = \frac{4\pi z^2 e^4}{m_0 V^2} \frac{NZ}{A} \ln \frac{2m_0 V^2}{I}, \text{ where}$$

$dE/dx$  = energy loss per unit length

$z$  = the atomic number of the projectile

$e$  = elementary charge  $4.803 \times 10^{-10}$  (erg-cm)<sup>1/2</sup>

$m_0$  = the electron rest mass

$V$  = relativistic projectile velocity

$A$  = Avogadro's number

$Z$  = atomic number of the target material

$I$  = adjusted ionization potential of the target material.

The stopping power of particles other than protons is given by the relationships:

$$\text{deuterons } S_d(E) = S_p(E/2)$$

$$\text{tritons } S_t(E) = S_p(E/3)$$

$${}^3\text{He } S_t(E) = 4S_p(E/3)$$

$${}^4\text{He } S_t(E) = 4S_p(E/4)$$

In order to have a useful accelerator target for the production of a radionuclide, it is necessary to effectively remove the heat generated by the passage of the beam. There are three modes of heat transfer which are active in

**Table 5** Radionuclides of current or potential use in therapy produced in nuclear reactors

	$T_{1/2}$	Nuclear reaction	Cross section (b)	Target
$^{32}\text{P}$	14.3 days	$^{31}\text{P}(\text{n}, \gamma), ^{32}\text{S}(\text{n}, \text{p})$	0.18, 0.06	$\text{KH}_2\text{PO}_4$ , sulfur
$^{35}\text{S}$	87.5 days	$^{35}\text{Cl}(\text{n}, \text{p})$	0.49	KCl
$^{64}\text{Cu}$	12.7 h	$^{63}\text{Cu}(\text{n}, \gamma)$	4.50	Enriched $^{63}\text{Cu}$
		$^{64}\text{Zn}(\text{n}, \text{p})$	0.039	Enriched $^{64}\text{Zn}$
$^{67}\text{Cu}$	2.6 days	$^{67}\text{Zn}(\text{n}, \text{p})$	0.001	Enriched $^{67}\text{Zn}$
$^{75}\text{Se}$	119.8 days	$^{74}\text{Se}(\text{n}, \gamma)$	48.0	Enriched $^{74}\text{Se}$
$^{89}\text{Sr}$	50.5 days	$^{88}\text{Sr}(\text{n}, \gamma)$	0.82	Enriched $^{88}\text{Sr}_2\text{O}_3$
$^{90}\text{Y}$	64.0 h	$^{235}\text{U}(\text{n}, \text{f})^{90}\text{Sr}$ $^{90}\text{Sr}(\beta^- \text{ decay})$	NA	Enriched $^{235}\text{U}$
$^{103}\text{Pd}$	16.99 days	$^{102}\text{Pd}(\text{n}, \gamma)$	3.4	Enriched $^{102}\text{Pd}$
$^{117\text{m}}\text{Sn}$	13.6 days	$^{117}\text{Sn}(\text{n}, \text{n}'\gamma)$	0.22	Enriched $^{117}\text{Sn}$
$^{114\text{m}}\text{In}$	49.5 days	$^{113}\text{In}(\text{n}, \gamma)$	8.1	Enriched $^{113}\text{In}$
$^{125}\text{I}$	60.1 days	$^{124}\text{Xe}(\text{n}, \gamma)^{125}\text{Xe}$ (ECdecay)	$>28.0^{\text{a}}$	Enriched $^{124}\text{Xe}$
$^{131}\text{I}$	8.04 days	$^{130}\text{Te}(\text{n}, \gamma)$	0.29	Enriched $^{130}\text{Te}$
		$^{235}\text{U}(\text{n}, \text{f})$	268 <sup>†</sup>	Enriched $^{235}\text{U}$
$^{153}\text{Sm}$	1.9 days	$^{152}\text{Sm}(\text{n}, \gamma)$	208	Enriched $^{152}\text{Sm}$
$^{166}\text{Ho}$	26.76 h	$^{165}\text{Ho}(\text{n}, \gamma)$	61.2	$^{165}\text{Ho}$ natural
$^{177}\text{Lu}$	6.7 days	$^{176}\text{Lu}(\text{n}, \gamma), ^{176}\text{Yb}(\text{n}, \gamma), ^{177}\text{Yb}(\beta^- \text{ decay})$	2090, 2.85	Enriched $^{176}\text{Lu}$ and $^{176}\text{Yb}$
$^{186}\text{Re}$	3.8 days	$^{185}\text{Re}(\text{n}, \gamma)$	112	Enriched $^{185}\text{Re}$
$^{188}\text{Re}$	17.0 h	$^{187}\text{Re}(\text{n}, \gamma)$	76.4	Enriched $^{187}\text{Re}$
$^{188}\text{W}$	69.78 days	$^{186}\text{W}(\text{n}, \gamma), ^{187}\text{W}(\text{n}, \gamma)$	36.5, 14.5 <sub>27</sub>	Enriched $^{186}\text{W}$
$^{195\text{m}}\text{Pt}$	4.02 days	$^{194}\text{Pt}(\text{n}, \gamma)$	0.042	Enriched $^{194}\text{Pt}$
$^{195\text{m}}\text{Pt}$	4.02 days	$^{195}\text{Pt}(\text{n}, \text{n}'\gamma)$	0.29 <sup>a</sup>	Enriched $^{195}\text{Pt}$
$^{198}\text{Au}$	2.7 days	$^{197}\text{Au}(\text{n}, \gamma)$	98.8	Gold metal
$^{199}\text{Au}$	3.14 days	$^{198}\text{Pt}(\text{n}, \gamma)^{199}\text{Pt}(\beta^- \text{ decay})$	3.66	Enriched $^{198}\text{Pt}$
$^{225}\text{Ac}$	10.0 days	$^{233}\text{U}$ decay	–	–

<sup>a</sup> unfiltered neutron spectrum

targets. These are conduction, convection, and radiation. Radiation is only a significant mode of heat loss at high temperatures ( $>500^\circ\text{C}$ ). Gases and liquids can transfer heat via convection and conduction. In most targets, the final removal of the heat will be from a backing plate to a flowing water stream. Heat transfer in solids is somewhat simpler than in other media since the heat usually flows through the target matrix mainly by conduction. Once the heat has been transferred to the cooled surface of the target, the heat will usually be removed by a fluid such as water flowing against the back of the target.

The transfer of the heat through the target material, and through the backing material, is fairly straightforward. The real surprises in designing solid targets come from the interfaces where the target material meets the backing material. This is where many problems arise and the better the connection one can make at this interface, the better the heat transfer will be. Problems with loss of target material or damage to the target during the irradiation will be less likely.

### 3 Reactor Production Using Neutrons

Table 5 lists some of the reactor-produced radionuclides important to therapeutic nuclear medicine. There are three general reaction types used: (a) neutron capture,  $[\text{n}, \gamma]$ ; (b) neutron capture followed by decay; and (c) fission. The most widely used route is the  $[\text{n}, \gamma]$  reaction with thermal neutrons. The advantage of this production process is its simplicity and high yield. It is straightforward in that in many cases elemental targets may be used and no chemical separation of target and product is required (or possible). Since cross-sections tend to be higher than most other reaction types, yields are generally good. The primary disadvantage of this reaction also relates to the fact that the radioactive product cannot be separated from the target. Thus, stable atoms dilute the radioactive atoms and the specific activity will be much lower than that of “carrier-free” or NCA radionuclide. Radioimpurities may arise from  $[\text{n}, \gamma]$  reactions on other isotopic forms of the target or

chemical impurities in the target. The use of isotopically enriched targets can minimize production of impurities and improve yield, but often at rather high costs. Nevertheless, enriched targets are essential if the natural abundance of the target isotope is low and significant impurities are co-produced.

In selected cases, there is a technique that can be utilized to improve the specific activity of  $(n, \gamma)$  produced radionuclides. This method is known as the Szilard Chalmers process (Mausner et al. 1989). The Szilard-Chalmers process depends upon the fact that, following neutron absorption, prompt gamma rays are emitted which may cause nuclear recoil and subsequent molecular bond disruption. This excitation sometimes leaves the resulting hot atom in a different chemical state from unreacted atoms and thus chemically separable. This separated fraction is relatively “enriched” in radioactive atoms and has higher specific activity than the rest of the target. The enrichment factor ( $E$ ) is the ratio of specific activity of recoiled fraction to that of the bulk irradiated target. The target in this case must be a compound which is thermally stable and resistant to radiolytic decomposition from fast neutrons and gamma rays. For example, the Szilard-Chalmers effect has been utilized with tetraphenyl tin to improve the specific activity of tin-117m (Mausner et al. 1992).

Another situation occurs as a result of an  $(n, \gamma)$  reaction, in which an intermediate radionuclide decays to the product of interest. This process is used to make I-125, for example, with the  $^{124}\text{Xe}[n, \gamma]^{125}\text{Xe} \rightarrow ^{125}\text{I}$  reaction. The neutron capture product Xe-125 beta decays with a 16.8 h half-life to I-125. Since the final product can be chemically separated from the target, specific activity approaching the theoretical value for pure radionuclide is possible. Obviously, using high chemical purity targets and processing reagents is necessary to avoid introducing stable isotopes of the same element in the product. In the I-125 example this means that both target and reagents should be free of stable iodine. It is also usually desirable to use an enriched target to minimize the co-production of long-lived or stable nuclides with the desired product. For example, irradiation of Xe-124 containing a few percent of Xe-126 (0.09 % natural abundance) will result in production of stable I-127 through the decay of Xe-127, and hence result in lower specific activity of the I-125 product. In this case, since the target and the product are chemically separable, it is possible and may be worthwhile to recover the rather expensive enriched target material for reuse (Mausner and Mirzadeh 2003).

A few useful radionuclides are produced with fast neutrons by  $[n, p]$  reactions (e.g., S-35, Sc-47, Cu-64, Cu-67), or by indirect reactions, such as that used for production of F-18. The  $[n, p]$  process shares many features with the  $[n, \gamma]$  reaction followed by beta decay process described above, since the target and product are chemically separable. The

indirect mechanism involves the use of an outgoing particle from an initial nuclear reaction to cause a second reaction in another target nucleus. For example, the neutron irradiation of Li-6 creates a triton ( $^3\text{H}$ ) with sufficient energy to react with a neighboring O-16 nucleus (in  $\text{Li}_2\text{CO}_3$ ) to form F-18, and the product is separable from the target(s) (Mausner and Mirzadeh 2003).

Neutron-induced fission of U-235 creates fission products with atomic numbers ranging from  $Z = 30$  to 66. For the purpose of radionuclide production, targets containing about 25 gm of highly enriched U-235 are irradiated and then chemically processed. Fuel rods also contain large amounts of U-235 and its fission products, but are not processed for their radionuclide content. Given the large number of radionuclides created by the fission process, the chemical procedures to recover the radionuclides of interest may be quite involved. The most important medical radionuclides produced by fission are I-131, Xe-133 and, of course, Molybdenum-99. The special role of Mo-99 and its daughter Tc-99m in nuclear medicine must be underscored (Richards et al. 1982; Srivastava 1996c).

---

## 4 Accelerator Production Using Charged Particles

As mentioned in the Introduction, the revival of interest in radionuclide therapy is a consequence of better tissue-specific and better molecularly targeted carriers for radioactivity and its ability to offer systemic treatments especially for disseminated (metastatic) disease in contrast to external beam treatment. However, the full potential of radionuclide therapy can only be achieved with the coupling of the most appropriate radionuclide for the clinical situation with a well designed highly selective carrier vehicle/biomolecule. Many relatively new radionuclides that are only producible in an accelerator, or can be done with better efficiency and lower cost with this approach, have been tested or proposed for these applications but scientific or practical hurdles have limited their use. Some of these issues and possible solutions will be discussed in the various sections to follow.

Despite the considerable progress in treating several types of tumors such as non-Hodgkin's lymphoma and others (as discussed in the various following chapters in this volume), radioimmunotherapy and radio peptide therapy of solid tumors is a more difficult problem. Part of the challenge is to couple the most appropriate radionuclide for the clinical situation. As mentioned earlier in this chapter, the prevalence or popularity of the utilization of I-131 and Y-90 for therapy is largely driven by their ready availability at reasonable cost rather than an analysis of optimization for the tumor. To summarize again, a desirable radionuclide should have particulate radiation (electron, or alpha) in

order to impart a high dose in a localized area. Other important physical parameters include the half-life, the energy, and emission abundance of the particles, and whether any gamma rays are also emitted. It is generally considered necessary to approximately match the physical half-life with the *in vivo* pharmacokinetics of the labeled agent. The important chemical issues to consider are the achievable radionuclide-specific activity, metal ion contamination, the clearance rate and affinity for body tissues of the free (and chelated) radionuclide, and the chemistry of attachment of the radionuclide to the carrier molecule, e.g., the MAb or peptide. Many excellent publications have reviewed the nuclear and chemical selection criteria to make this decision (Srivastava 1988; Mausner and Srivastava 1993), the production methodology (Volkert et al. 1991), and dosimetric/biological considerations (Srivastava 1996b; Neves et al. 2005; O'Donoghue et al. 1995; Carlsson et al. 2003). It is unlikely that there is a single optimum radionuclide for all tumor types or sizes. The major scientific and practical impediments that have hindered research and clinical use of many attractive therapeutic radionuclides are issues that include matters of radionuclide quantity, quality (purity and specific activity), a continuous reliable availability, and distribution.

---

## 5 Targetry

Upon determining the production reaction and irradiation conditions, one must select an appropriate target material. Whether for use in a reactor or accelerator (cyclotron), there are several general factors to be considered:

### 5.1 Physical and Chemical Form

Pure metals or elements are generally best. If not suitable due to the constraints below, favorable materials include alloys as well as simple compounds such as oxides, carbonates, halides, etc. This form must also be compatible with post-irradiation processing. Thus, easily dissolved compounds are sometimes preferable over metal targets.

### 5.2 Thermal Properties

There can be substantial sample heating during irradiation. Incident particles impart energy and some nuclear reactions are exothermic. Although thermal neutrons do not transfer much energy, fast neutrons can. Additionally, some of the energy of prompt gammas from  $[n, \gamma]$  reactions generated in the sample, fuel elements, reactor containment, and other nearby samples can be absorbed in the sample. The

“gamma eating” is proportional to sample mass and can be substantial for samples in excess of a gram. Charged particles lose energy rapidly in a sample. The power in watts is equal to the energy deposited (MeV) multiplied by the beam current (in  $\mu\text{A}$ ). For example, a thick target which degrades a proton beam 15 MeV at 100  $\mu\text{A}$ , absorbs 1,500 W in a few square centimeters. Target cooling is thus essential in accelerators in order to prevent target overheating and possible destruction. In addition, the target material should have good thermal conductivity and a high melting point. For these reasons organic compounds and aqueous solutions cannot usually be used.

### 5.3 Chemical Stability

The target must not decompose at elevated temperature or evolve gases that would pressurize and rupture the containment capsule. Also, the target should not react with the encapsulating material. Finally, the sample must not be substantially decomposed by radiation damage. This is hard to predict *a priori*. This requirement generally excludes all organic material as a target for large-scale production of isotopes.

### 5.4 Purity

Targets with high radionuclide purity are often necessary to minimize radiocontaminants due to the activation of impurities. In compounds, the activation of all atoms must be considered. Sometimes, isotopically enriched material is necessary to suppress competing reactions on other naturally occurring isotopes in the target. To achieve high specific activity, the amount of element of the final product in the target is crucial. For example, the Cu content of ZnO targets for Cu-67 production must be  $<0.1$  ppm.

### 5.5 Encapsulation

For safety and to prevent cross-contamination, the target is almost always sealed in a primary container. For reactor irradiation at low neutron flux and short periods, small plastic tubes are useful as they do not activate appreciably and are inexpensive. At the higher neutron flux and longer irradiation time used for isotope production, samples are typically encapsulated in high purity quartz ampoules. These quartz ampoules are often placed in  $\gamma$  holders specific to the irradiation facility. The much higher level of energy dissipation in accelerators makes the construction of targets rather complicated (Weinreich 1992).

## 5.6 Availability

The target material should be readily available commercially in high purity.

## 5.7 Target Transport Systems

Capability for the production of short-lived radioisotopes in a nuclear reactor is another important criterion to be considered. Access to the reactor irradiation facilities during reactor normal operation allows short irradiation periods, which are required for the production of many useful short-lived radioisotopes such as Sc-47, Cu-64, Cu-67, Rh-105, Pd-109, Sm-153, Ho-166, and Au-199. These isotopes all have half-lives of about 3 days or less. Production of Mo-99 can also be enhanced by online access to the targets.

The pneumatic tube facilities are typically used for irradiation of small samples in plastic or graphite capsules for accurate time intervals of a few seconds to 10 min or longer depending on the neutron or gamma heating of the facility. The pneumatic facilities are typically located in the reflector region of the reactor, and the capsule loading and unloading station is located in the experiment room of the neutron activation laboratory. The capsules are inserted into the reactor and returned to the laboratory using compressed air.

The online access to the reactor irradiation facilities can be accomplished pneumatically, hydraulically and by the use of vertical thimbles. A hydraulic “rabbit” permits for insertion and removal of samples while the reactor is operating. The water pressure-drops that exist in the primary coolant system are typically utilized as the driving forces for moving the capsules through the system. Normally, the heat flux at the surface of the capsule, due to neutron and/or gamma heating of the capsule and its contents, is limited. For the hydraulic tube facility in the HFIR at ORNL, this limit is of the order of  $2 \times 10^2 \text{ kWm}^{-2}$  per capsule. In addition, the neutron poison content of the facility load is limited such that the reactor is not subjected to a significant reactivity change during the insertion or removal of capsules.

Thimble mechanisms allow access to the reactor simply by attaching the irradiation capsule to the end of long aluminum tubing and lowering the capsule into the reactor and to withdraw it after the irradiation. The thimbles are fitted with a set of reentrant tubes connected to a separate cooling system which circulates a flow of 10 or more l/min downward through the center and upward through the outer annular region of each tube. Samples are placed in aluminum capsules which are immersed in the cooling water, or thimble tubing can be used to vent the capsule, to fill it with gas for heat transfer, and to bring out a pair of thermocouple leads, if desired.

## 6 Radiochemical Processing and Purification

Except for  $[n, \gamma]$  reactions in a reactor, most radionuclides require chemical separation from the target material and induced radioactive by-products. Generally, one or more of conventional techniques, such as chromatography, solvent extraction, distillation, and precipitation are used. Other techniques include electrolysis and electro-deposition, and separations based on sublimation. These processing techniques are adapted to the unique requirements of radiochemistry—the hazards of radiation exposure and contamination, rapid separation times in order to minimize decay losses, and the separation of essentially massless (carrier-free or ‘no-carrier-added’, NCA) amounts of product from bulk target. A great deal of effort has gone into developing processes suitable for each individual application.

### 6.1 Solvent Extraction

This technique involves the selective partitioning of particular chemical complexes between two immiscible solvent phases. Usually an aqueous solution of acid, base, or salt and an organic solvent such as ketone, ether, amine, or carbon tetrachloride are used. Its use in radiochemistry is partly due to the fact that partition coefficients are approximately independent of concentration down to tracer levels. It is also relatively simple and rapid to perform, can be extremely selective, and can be adapted to remote or automated operation. Extraction of a complex containing the radionuclide into the organic phase is often followed by evaporation or a back extraction into an appropriate aqueous phase. For example, extraction of Ga (III) and In (III) chlorides into isopropyl ether followed by evaporation of the ether or back extraction is a commonly used approach that has been adapted for Ga-67 and In-111 purification (Brown 1971, 1972). The variables to be controlled are pH, relative phase volumes, salt concentration, and mixing time.

### 6.2 Chromatography

This method is one of the most powerful and widely used for radiochemical separations, especially ion exchange. It is related to solvent extraction in that it depends upon the differential distribution of a species between two phases, except that in chromatography the phases move relative to one another. In ion exchange the distribution of an element between a solution (mobile phase) and stationary resin (usually packed in a column) depends on the ionic form, the

solute concentration, and the functional group on the resin. Cation exchangers such as Dowex 50 have sulfonic acid groups, while in anion exchangers such as Dowex 1 the functional group is quaternary amine groups. Once a resin type is chosen, the variables to be controlled are ionic concentration, column volume and diameter, flow rate, and eluant. With proper choice of conditions, ion exchange is very useful for separating carrier-free radionuclides from bulk target (mass ratio  $>10^8$ ) having significantly lower affinity toward the resin. This method has been particularly successful in separating transition metals from each other and from the rare earth elements. A relevant example is the separation of Co-55 from Fe target (Lagunas-Solar and Jungerman 1979). It can be combined with solvent extraction for better separation factors, as was demonstrated in the case of Cu-67 (Dasgupta et al. 1991). It is also readily adaptable to remote or automated operation.

### 6.3 Distillation

Some radiochemical separations can be affected by exploiting differences in volatility. For example, I-131 can be separated from Te targets by dry distillation at high temperature (Evans and Stevenson 1956) or from a dissolved target (Hupf 1976). One can also distil the target away from the product, as was done to separate P-32 from an elemental sulfur target (Evans and Stevenson 1957; Mani and Majali 1966). However, most therapeutic radionuclides of interest in this chapter except perhaps tin-117m are not amenable to this type of purification.

### 6.4 Precipitation

In radiochemistry, precipitation plays less of a role than other separation applications. This is because of the carrier-free nature of the radionuclides—there is simply not enough mass to precipitate. Reversing the process, that is, precipitating the bulk target away from the product is sometimes used, but may still cause problems by carrying down the desired product by mass effects. Though occasionally useful for a first bulk separation or for low specific activity radionuclides, precipitation rarely has the desired selectivity for therapeutic nuclear medicine requirements. Adsorption on walls of glassware and filter paper can be troublesome, and handling precipitates under remote conditions may be difficult.

### 6.5 Shielded Facilities

The handling and processing of reactor or accelerator produced radionuclides has to be carried out in specially

designed radiochemistry laboratories with controlled ventilation and air conditioning, shielded remote handling facilities, and radioactive waste collection and storage tanks (Mausner 1999). In most cases involving processing of reactor or cyclotron targets, radiation shielding for the chemist is required. This may be as simple as some stacked lead bricks inside a standard chemical fume hood. For pure beta emitters, small Lucite disks mounted on tongs to shield the hands are all that is necessary. At higher levels of gamma radiation, a completely enclosed hot box or hot cell will be required. Hot cells usually have 4–8 inches of lead in the walls or several feet of concrete, lead glass windows, and master–slave manipulators.

### 6.6 Current Requirements and Challenges

Specific activity, as mentioned earlier, is an important parameter since in many cases the availability of very high specific activity or NCA radioisotopes is required for biological applications. Specific activity is defined as the relative abundance of a radioactive isotope to the stable isotopes of the same element in a homogeneously mixed sample. Specific activity is usually expressed in terms of the disintegration rate per unit mass of the element (e.g. mCi/mg). One example of the importance of high specific activity is the radiolabeling of tumor-specific antibodies for both diagnostic and therapeutic applications where only very small amounts of the radiolabeled antibodies are administered to ensure maximal uptake at the limited tumor cell surface antigen sites. Another example is the use of receptor-mediated radiopharmaceuticals that are potentially very important for the clinical evaluation of hormonal or neurological diseases. Since the population of hormones and neurotransmitter sites is very limited, high specific activity agents are required to ensure maximum site-specific uptake.

Since the specific activity of a radioisotope produced by particle-induced reactions is a direct function of the incident particle flux, an increase in the incident particle flux results in an absolute increase in the specific activity of the product. This relationship is linear for simple reactions and nonlinear for complex reactions. It is important to note that the half-lives, production and destruction cross-sections, and irradiation time are equally important.

Several important radioisotopes have long physical half-lives and low production cross-sections requiring long irradiation periods even in the highest neutron flux available. Examples in this category include tungsten-188 (half-life 69 days; parent for rhenium-188; vide infra).

In addition, the increased flux not only results in higher specific activity products but will result in conservation of the enriched target material. For example, increase of the

**Table 6** Reactor production of no-carrier-added<sup>67</sup> Cu

Reactor/Position	Fast neutron flux ( $E_n \geq 1$ MeV) ( $n \cdot s^{-1} \cdot cm^{-2}$ )	Sat. Yield of <sup>67</sup> Cu at EOB ( $\mu Ci/mg$ of <sup>67</sup> Zn)	Cross-section, (mb)
HFIR (85 MW) Hydraulic tube	$4.4 \times 10^{14}$	$110 \pm 10$	$1.07 \pm 0.11$
<sup>a</sup> HFBR (60 MW) In-core, V15 Core-edge, V11	$3.0 \times 10^{14}$ $6.4 \times 10^{13}$	$90.2 \pm 9.5$ $14.4 \pm 1.6$	$1.23 \pm 0.13$ $0.91 \pm 0.10$

<sup>a</sup> Now closed down

**Table 7** Accelerator (charged particle)—produced therapeutic radionuclides

Radionuclide	Half-life	Decay mode	Nuclear reaction
<sup>67</sup> Cu	2.6 days	EC	<sup>70</sup> Zn(p, $\alpha$ ), <sup>68</sup> Zn(p, 2p), <sup>78</sup> Se(p, 2n)
<sup>77</sup> Br	56 h	EC	<sup>79</sup> Br(p, 3n) <sup>77</sup> Kr, <sup>75</sup> As( $\alpha$ , 2n)
<sup>81</sup> Rb	4.6 h	EC	<sup>82</sup> Kr(p, 2n)
<sup>111</sup> In	2.8 days	EC	<sup>112</sup> Cd(p, 2n)
<sup>67</sup> Ga	78.3 h	EC	<sup>66</sup> Zn(p, n)
<sup>103</sup> Pd	17.0 days	EC	<sup>103</sup> Rh(p, n)
<sup>124</sup> I	4.18 days	EC, $\beta^+$	<sup>124</sup> Te(p, n), <sup>125</sup> Te(p, 2n), <sup>124</sup> Te(d, 2n)
<sup>201</sup> Tl	3.06 days	EC	<sup>203</sup> Tl(p, 3n) <sup>201</sup> Pb- $\beta$ decay
<sup>211</sup> At	7.2 h	$\alpha$	<sup>211</sup> Bi( $\alpha$ , 2n)
<sup>225</sup> Ac	10.0 days	$\alpha$	<sup>226</sup> Ra(p, 2n)

**Table 8** Production of Sc-47 in BLIP via <sup>nat</sup>Ti(p,spall) reactions

Run	Incident proton energy (MeV)	Target thickness (mm)	Yield <sup>a</sup>	Radioimpurity ratios at EOB (fractions of Sc-47)		
				Sc-44	Sc-46	Sc-48
Theoretical	200	2.5	10.9 GBq	0.49	0.08	0.02
BLIP	192	0.127	118.0 MBq	0.50	0.09	0.16
Theoretical	35	17.4	6.8 GBq	0.90	0.05	0.04

<sup>a</sup> 3.35-day irradiation, 50  $\mu A$  beam current

neutron flux by a factor of two requires only about half of the enriched target material to produce the same amount of radioactive product. Considering the limited availability of the enriched materials, conservation is necessary. Sometimes a higher flux, particularly in reactor production, increases the potential capacity of the reactor by reaching the equilibrium conditions quicker.

## 7 Production of Selected Therapeutic Radionuclides

Many reactor as well as accelerator-produced radionuclides have been tried and proposed for various types of radionuclide therapies. A list of these radionuclides of current interest to nuclear medicine is presented in Tables 5, 6, 7, and 8, together with their mode of production and their corresponding nuclear cross-sections. From these lists, the

production and chemical processing of the following radioisotopes important in nuclear medicine for therapeutic oncology and other therapeutic applications, representing different types of nuclear reactions, is discussed in some detail: beta emitters scandium-47, copper-67, yttrium-86 (positron emitter surrogate for yttrium-90), holmium-166, lutetium-177g, and the tungsten-188/rhenium-188 system, alpha emitters astatine -211 and the actinium-225/bismuth-213 system, and Auger and conversion electron emitters tin-117m, platinum-195m, and mercury-195m.

Most efforts to date have involved beta emitting isotopes as they offer a wide range of chemical and nuclear properties and potentially can be used in many types and sizes of tumors. Among the more popular recent candidates are Cu-67, Lu-177, and Rhenium-188. All have notable advantages but some disadvantages as well. The enhanced radiobiologic toxicity of alpha emitters due to high linear energy transfer ( $\sim 100$  keV/ $\mu m$ ) and short path length in

tissue (50–80  $\mu\text{m}$ ) can deliver more specific tumor cell killing with less damage to normal tissues than beta emitters and seem ideal to treat minimal residual disease or micrometastases. This has sparked renewed interest in using these isotopes for radioimmunotherapy of micrometastatic disease and disseminated cancers such as leukemia. Of these candidates, At-211 and Ac-225/Bi-213 have received the most attention. They too have some practical disadvantages. Finally, several investigators are trying to utilize the very high LET and very short range of Auger electrons for cancer therapy using molecular carriers that internalize the isotope in the cell mitochondria or nucleus. Almost all nuclides which decay by electron capture and isomeric transition emit low energy electrons. This includes some isotopes routinely used in imaging applications, for example In-111, Ga-67, and Tl-201, and possibly others such as Tm-171m. For example, the conversion electron and Auger energy per decay in In-111 is  $7.40\text{E-}02$  g-rad/ $\mu\text{Ci-h}$ , for Ga-67 it is  $7.29\text{E-}02$  g-rad/ $\mu\text{Ci-h}$ , and for Tl-201 it is  $9.21\text{E-}02$  g-rad/ $\mu\text{Ci-h}$ . In contrast, the highest Auger yield is exhibited by Pt-195m with  $3.90\text{E-}01$  g-rad/ $\mu\text{Ci-h}$  of energy per decay. Also of interest are Hg-195m and Sn-117m, emitting the very impressive  $2.94\text{E-}01$  g-rad/ $\mu\text{Ci-h}$  and  $3.43\text{E-}01$  g-rad/ $\mu\text{Ci-h}$  of short range energy, respectively (Weber et al. 1989).

## 7.1 Beta Emitters

### 7.1.1 Scandium-47

Two low-energy reactions in the reactor that produce NCA Sc-47 are  $^{47}\text{Ti}(n, p)^{47}\text{Sc}$  and  $^{46}\text{Ca}(n, \gamma)^{47}\text{Ca}(\beta^-)$  ( $t_{1/2} = 4.54$  days) (Mausner et al. 1993). The former reaction requires  $E_n > 1$  MeV, while the latter reaction uses thermal neutrons. Both types of neutrons are available in the fission neutron spectrum in the High Flux Isotope Reactor at Oak Ridge National Laboratory. The advantages of the  $^{46}\text{Ca}(n, \gamma)^{47}\text{Ca}(\beta^-)$  reaction are: (1) the year-round availability of high flux thermal neutrons; and (2) use of a Ca-47/Sc-47 generator system to supply Sc-47 activity. The disadvantage of this route is the requirement of an enriched target. Calcium-46 is presently available with only a 30 % enrichment and at a very high price, which makes target costs prohibitive.

The  $^{47}\text{Ti}(n, p)$  route also requires an enriched target though  $^{47}\text{Ti-O}_2$  is available with very high enrichment (94.53 % Ti-47, 4.74 % Ti-48, 0.35 % Ti-46, 0.2 % Ti-49, and 0.18 % Ti-50) and at more reasonable cost. The hydraulic tube positions at HFIR at ORNL (with  $4.6 \times 10^{14}$  neutrons/ $\text{cm}^2\text{s}$ ) have adequate flux in the high-energy region of the neutron spectra to produce sufficient quantities of Sc-47 activity for theragnostic applications in

radioimmunotherapy. The reported cross section in a fission neutron spectrum is 18.9–26 mbarn, which is comparable to the cross-section value for proton-induced reactions such as  $^{nat}\text{Ti}(p, 2p)$  and  $^{51}\text{V}(p, 3pn)$  (Kolsky et al. 1998).

Several  $^{47}\text{TiO}_2$  targets were irradiated at HFIR for periods ranging from a few hours to several days (Hnatowich 1990). The experimental results are lower than the theoretical ones, perhaps due to differences in the actual neutron spectrum when the irradiations occurred compared to the theoretical neutron spectrum. High production yields using the PTP positions at the HFIR were obtained. These results indicate that Sc-47 can be produced at a reactor using the  $^{47}\text{Ti}(n, p)$  reaction in quantities sufficient for theragnostic applications. For example, at HFIR a 3.35 days (one half-life of Sc-47) irradiation of a 10 g target would theoretically produce  $\sim 75$  Ci of Sc-47 at EOB. Both the Sc-46/Sc-47 and Sc-48/Sc-47 impurity ratios are less than 0.4 % at EOB (end of bombardment), leading to a product with greater than 99.5 % radiopurity (Mausner et al. 1993; Kolsky et al. 1998).

The specific activity of Sc-47 depends essentially on the scandium content of the enriched target material. Scandium is not a ubiquitous contaminant such as lead or copper, and would not be expected to be introduced during processing of the target. These expectations were borne out when several product samples were analyzed with ICP-AE and no stable Sc was detected (Kolsky et al. 1998). Since scandium was not detected in batches of target material, stable scandium content can be assumed to be the reported detection limit. The specific activities are high enough for antibody labeling applications in radioimmunotherapy. Conservatively, assuming that an average of two to three scandium-ligand complexes can be attached to each antibody molecule without loss of immunoreactivity, up to 30 mCi (1.16 GBq) of ORNL produced Sc-47 can be used to label 1 mg of a typical IgG antibody (mol. wt.  $\sim 150$  kdalton) given the measured specific activities (Kolsky et al. 1998).

Finally, it is necessary to recycle the expensive enriched target material to defray the target cost over many production runs. A simple procedure was developed that recovers  $\sim 98.5$  % of the oxide based on precipitation of titanium at basic pH followed by conversion to the oxide using higher temperature (Kolsky et al. 1998). Titanium may be recovered and easily reused since the only titanium activation product is the short-lived Ti-51 ( $t_{1/2} = 5.8$  min) produced by the  $^{50}\text{Ti}(n, \gamma)$  reaction using thermal neutrons. Other radionuclidic impurities that have been detected in recycled material are Ta-182 ( $t_{1/2} = 114.4$  days) and Zn-65 ( $t_{1/2} = 244$  days). These isotopes are also produced by (n,  $\gamma$ ) reactions on minor target impurities of stable Ta and Zn. If required, these impurities could easily be separated from the target material using anion-exchange chromatography before precipitation of the titanium (Kolsky et al. 1998).

**Table 9** Sc-47 versus Cu-47 as a therapeutic radiolabel

	Cu-67		Sc-47	
	Advantages	Disadvantages	Advantages	Disadvantages
Half-life	Good (2.58 days)	–	Good (3.35 days)	–
Beta energy, keV (total, weighted avg.)	Good (141)	–	Good (163)	–
Imageable photon (keV, %)	Good (185, 49 %)	–	Good (159, 68 %)	–
Specific activity	–	Low (2–18 mCi/μg)	High (no-carrier added)	–
Radiochemistry	–	Average	Good	–
Radiochemistry	–	Hard (accelerator)	Easy (reactor)	–

Relative production yields were also determined using the (p, 2n) reaction on  $^{48}\text{TiO}_2$  targets (98.5 %  $^{48}\text{TiO}_2$ ) at the BLIP in the energy region  $48 < E_p < 150$  MeV (Srivastava 2011; Srivastava and Dadachova 2001; Mausner et al. 1993, 2000; Kolsky et al. 1998). These targets were irradiated to see whether the use of isotopically enriched Ti-48 would improve the Sc-47/Sc-44m, 46, 48 radioimpurity ratios compared to using natural Ti targets. There is the expected improvement in the Sc-47/Sc-44 ratios using enriched targets since the  $^{49}\text{Ti}(p,2p)^{48}\text{Sc}$  and  $^{50}\text{Ti}(p,2pn)^{48}\text{Sc}$  reaction pathways have been eliminated. The Sc-47/Sc-44m ratio is better at lower irradiation energies ( $E_p < 100$  MeV); however, unfortunately the Sc-47/Sc-46 ratios are worse throughout the energy region measured. Thus, this production method would not be suitable for producing Sc-47 with sufficient purity for therapeutic use (Kolsky et al. 1998).

Although Cu-67 has long been considered as one of the ideal therapeutic/theragnostic radionuclides (vide infra), its scaled-up production with a sufficiently high specific activity is still an issue that has only partially been resolved and further improvements are difficult if not questionable, at this time. With this in mind, we have proposed Sc-47 as a possible replacement for Cu-67 (Mausner et al. 2000), as shown in Table 9.

### 7.1.2 Copper-67

Copper-67, with a 2.6-day half-life, is the longest lived radioisotope of Cu (Mirzadeh et al. 1986). It provides medium-energy emission of  $0.6 \text{ MeV}_{\text{max}}$  (average, 141 keV), photon emissions (184 keV, 48.7 %; 93 keV, 16 %; 91 keV, 7 %), and facile labeling chemistry. It is a very attractive theragnostic radionuclide (Srivastava 2009, 2010, 2011, 2012). The half-life is suitable for imaging slow in vivo pharmacokinetics with agents such as MAbs and other carrier molecules, and the beta particle energy is appropriate for therapy. The 184-keV gamma ray permits

imaging of the uptake and biodistribution of the agent both before and during therapy administration. It can also be paired with the positron emitter Cu-64 to perform pre-therapy biodistribution determinations and dosimetry by PET. However, as mentioned earlier in this article, the use of Cu-67 has been inhibited by a lack of regular availability of sufficient quantities at a cost that researchers can typically afford, as well as the low specific activity issue (Srivastava and Dadachova 2001; Mirzadeh et al. 1986). In the past several decades, the most typical source in the United States has been the high-energy proton irradiation of natural Zn targets (Mirzadeh et al. 1986), primarily irradiated at either the Brookhaven Linac Isotope Producer (BLIP) at BNL or at the Isotope Production Facility (IPF) at Los Alamos National Laboratory (LANL). These are both large accelerators operated and funded for physics research only part of each year. Thus, in the past, it has not been possible to provide Cu-67 on a time frame suitable to support clinical trials, with the attendant schedule fluctuations and changing patient status (DeNardo et al. 1998, 1999). Additionally, the specific activity was at the low end of what was acceptable for antibody therapy, ranging from about 5–10 Ci (185–370 GBq) per mg of Cu at EOB. With the construction of a new target station at the IPF at LANL in 2004, the beam intensity and production have improved, but year-round availability still cannot be assured. Recent studies at BNL have tried to determine the causes of the low specific activity (Medvedev et al. 2012). Exhaustive assays of all the reagents used in processing determined that these contribute only approximately  $0.3 \mu\text{g}$  of Cu. Addition of the ZnO target to these blank experiments contributed only another  $1.4 \mu\text{g}$  of Cu. This compares with the  $25 \mu\text{g}$  of Cu typically measured in a batch of 80–380 ( $\sim 3$ – $14$  GBq) of Copper-67. This result implies that most of the stable Cu found in each batch is produced directly by proton nuclear reactions on Zn, an often forgotten process. To investigate this hypothesis further, theoretical calculations of stable Cu

isotopes were attempted using the well-known nuclear radiation transport code MCNPX. The predicted direct production of stable Cu-63 was approximately 11  $\mu\text{g}$ , and 1  $\mu\text{g}$  of stable Cu-65, for every 200mCi ( $\sim 7.4$  GBq) of Cu-67 produced. Therefore, this route is the major source of the reduction in specific activity and will be very difficult to remove. Because Cu-63 is likely produced by the  $^{64}\text{Zn}(p,2p)$  and  $^{66}\text{Zn}(p,3p)$  reactions, use of a highly enriched Zn-68 target containing minimal Zn-64,66 may suppress the Cu-63 production. Recent accurate cross-section measurements on the  $^{68}\text{Zn}(p,2p)^{67}\text{Cu}$  reaction performed radiochemically over the energy range of 30–70 MeV showed that the yield of Cu-67 is fairly high (Dadachova et al. 1995). Unfortunately, Zn-68 is rather expensive. Also, recycling the target material is considered difficult because of the unavoidable co-production of long-lived Zn-65 in the target, unless the proton energy is kept around 70 MeV. To try to resolve these issues, BNL has recently been engaged in further research to develop the production of Cu-67 using high-energy proton irradiation of enriched Zn-68 targets, followed by selective chemical separation of the pure product (Medvedev et al. 2012). A number of specific challenges were addressed: (1) development of very thick electroplated Zn-68 disks as targets; (2) development of recovery/reuse technique of this expensive material after radiochemical processing; (3) development of a target capsule that can be sealed and then opened remotely in a hot cell; (4) development of a rapid highly selective chemical separation process for Cu-67; and (5) performing irradiations and measurements of product radiopurity, chemical purity, and labeling efficiency. This research has allowed the prospect for the production capability for Cu-67, using a high beam-current accelerator or cyclotron, in sufficiently large quantities and with a greater than five times of the previously obtained specific activity, to support clinical trials (Medvedev et al. 2012).

### 7.1.3 Yttrium-86

The popular beta-emitter therapeutic isotope Y-90, which is part of the Food and Drug Administration-approved radioimmunotherapy agent Zevalin (Spectrum Pharmaceuticals, Inc, Henderson, NV), has no imageable gamma photon in its emission. However, Y-86, a positron emitter ( $E\beta^+ = 660$  keV, 33 %) with a  $t_{1/2}$  of 14.74 h, could be a good choice as a surrogate pre-therapy PET imaging congener for Y-90 (Srivastava 2009, 2010, 2011) for various Y-90 based therapeutic radiopharmaceuticals including Zevalin. Although there are several high-energy gamma particles in its emission ( $E\gamma$ , keV: 1076.6, 82.5 %; 627.7, 32.6 %, and many others), which contribute to increased patient dose with no benefit, for cancer patients, who are

candidates for radioimmunotherapy, the imaging dose would generally not be considered as a major issue of concern.

The possible production routes for Y-86 that have been considered are as follows:  $^{86}\text{Sr}(p, n)^{86}\text{Y}$ ,  $E_p = 14.5 \rightarrow 11.0$  MeV;  $^{\text{natRb}}(3\text{He}, xn)$ ,  $E \text{ } ^3\text{He} = 24 \rightarrow 12$  MeV;  $^{88}\text{Sr}(p, 3n)^{86}\text{Y}$ ,  $E_p = 45 \rightarrow 37$  MeV; and  $^{90}\text{Zr}(p, 2p3n)^{86}\text{Y}$ ,  $E_p = 40 \rightarrow 30$  MeV (Srivastava 2010, 2011, 2012; Herzog et al. 1993). Out of these, it seems that the best method is the  $^{86}\text{Sr}(p, n)^{86}\text{Y}$  reaction, but it requires enriched  $^{86}\text{Sr}$ , which is rather expensive, and economy requires its recovery and reuse (Herzog et al. 1993; Sadeghi et al. 2009; Medvedev et al. 2011). Recovered Sr-86 will contain radioactive Sr-85 after first irradiation if the proton energy is more than 14 MeV, which would mean that hot cell target assembly will be required. At BNL, we have designed such a target, both halves of which are aluminum for better conductivity, head screws are large enough for remote manipulator handling, and silver-coated stainless steel C-rings are used to provide adequate seals (Medvedev et al. 2011). Such a target design was successfully irradiated in the BLIP without any leakage and can be opened and sealed in a hot cell.

Modification to increase active area in beam may increase production levels but will require more enriched Sr-86 to be used. However, if really a low energy of 14 MeV is used, the amount of target material needed is not high. Targets of both natural SrCl<sub>2</sub> and enriched SrCl<sub>2</sub> were irradiated yielding 10–13 mCi/ $\mu\text{Ah}$  of Y-86, giving an EOB batch yield of  $\sim 1,000$  mCi in 1 h, which is quite high (Medvedev et al. 2011). Chemical yields of Y-86 ranged from 82 to 93 %, and a further improvement is desirable. For labeling purposes, this chemical purity allowed for a labeling yield of 84 %, and this needs to be improved further as well. The level of a major radionuclidic impurity, Y-87 m, was a disappointing 34–55 %. The low-energy route on enriched Sr-86, which has previously been used (Srivastava 2011; Herzog et al. 1993) has allowed for better material and is now being pursued at BNL for larger-scale production. At BLIP, our first irradiation gave very low yield because the beam spot was larger than the target area. Also, the lowest tunable beam energy at the BLIP is 65.5 MeV, but the nuclear reaction cross-section peak is at  $\sim 14.5$  MeV. The choice of degraders seems to have resulted in too high a target entrance energy. BLIP is not an ideal facility for this low-energy reaction, but we carried out these investigations mainly to produce some material to develop a better and quicker radiochemical processing methodology that was short enough to allow for same-day irradiation and shipment, which has recently been accomplished (Medvedev et al. 2011).

### 7.1.4 Holmium-166

Holmium-166 (Ho-166) is utilized in medical radiotherapeutic applications due to its physical properties which include high-energy beta radiation [ $E_{\beta 1} = 1,855$  keV (51 %),  $E_{\beta 2} = 1,776$  keV (48 %), and  $E_{\beta}^{\text{av}} = 666$  keV], a 26.4 h half-life and decay to a stable daughter. In addition, Ho-166 has chemical characteristics suitable for protein labeling with bifunctional chelates. Holmium-166 also emits low intensity and low energy gamma rays (80.5 keV, 6 %) which are suitable for imaging. Due to the absence of high energy gamma rays in its decay, Ho-166 may be used for outpatient therapy without significant external radiation to other individuals (Dadachova et al. 1995, 1997; Smith et al. 1995).

Although Ho-166 with moderate specific activity can be produced by the  $^{165}\text{Ho}[\text{n}, \gamma]^{166}\text{Ho}$  reaction, its radionuclidic parent, Dy-166 ( $t_{1/2} = 81.5$  h), can serve as a source (generator) of high specific activity Holmium-166. Dysprosium-166 is produced by the double neutron capture reaction on Dy-164. As mentioned earlier, in certain applications, such as protein labeling, the use of a high specific activity radioisotope is essential. In addition, generator-produced Ho-166 is free from 1200-y Ho-166 m which is unavoidably co-produced with Ho-166 by the  $^{165}\text{Ho}[\text{n}, \gamma]$  reaction. For a four-day irradiation of 13.3 mg of natural Ho (monoisotopic) as  $\text{Ho}_2\text{O}_3$  at the position 5 of HT-HFIR at ORNL, the experimental yield of Ho-166 is 96.5 Ci, in comparison to the theoretical yield of 75.7 Ci. Therefore, the specific activity of Ho-166 at saturation at the end of bombardment would be  $\sim 10$  Ci/mg of Ho-165. The experimental yields of Dy-166 are 3.5 and 2.2 Ci/mg of Dy-166 for 8 and 1-day of irradiation in positions 5 and 6 of HT-HFIR at ORNL, respectively. Although the yield of the indirect route is lower than the direct route by a factor of 3, the specific activity of carrier-free Ho-166 produced from beta decay of Dy-166 would be much higher—depending on the degree of separation between Dy and Holmium. Because of the uniform chemistry exhibited throughout the lanthanide series, the separation factors between the adjacent members, however, are not very large. The reverse phase ion exchange chromatography technique has been used extensively for separation of various members of lanthanides, and the applicability of this technique for the separation of carrier-free Ho-166 from mg quantities of Dy has been shown (Dadachova et al. 1994). In reverse phase ion exchange chromatography, Ho and Dy are partitioned between the cation exchange resin (AG 50 W or Aminex-A5) and the mobile phase containing the weakly complexing ligand  $\alpha$ -HIBA at pH 4.3–4.6. As a consequence of “lanthanide contraction” and smaller ionic radii, the complex of  $\alpha$ -HIBA with Ho has slightly higher thermodynamic stability than that with Dy, and the elution pattern is reversed with Ho being eluted first. The log  $\beta$  (overall

stability constant) of Ho and Dy complexes with  $\alpha$ -HIBA are 7.67 and 7.24 at 0.1 ionic strength, respectively (Dadachova et al. 1994). Under optimum conditions of [ $\alpha$ -HIBA] = 0.085 M, pH = 4.27, T = 25 °C and flow rate of 0.8 mL/min, quantitative separation between Ho and Dy was achieved in a metal-free HPLC column containing Aminex-A5 resin operated at 1400 psi, with a separation factor of  $\sim 1,000$ . Further separation of the purified Ho-166 from  $\alpha$ -HIBA was achieved with a small column of AG 50W  $\times$  12 from 1 M HCl solution followed by elution of the ionic  $\text{Ho}^{3+}$  from column with 6 M HCL (Dadachova et al. 1994).

### 7.1.5 Lutetium-177g (Lu-177)

The direct production by thermal neutron irradiation of Lu-176 is simple, produces large quantities of Lu-177g (Lu-177, used interchangeably) because of a very large reaction cross-section of 2090 barns, and also relatively little burn-up of Lutetium-177 (Mausner and Mirzadeh 2003). There is only a small amount of the long-lived isomer Lu-177m (160.1d), which is co-produced. Therefore, Lu-177 is relatively inexpensive to make in a research reactor. It is inherently a low specific activity route but with the high thermal neutron flux available at some US and Russian reactors, specific activity of 68–75 Ci ( $\sim 2,500$ – $2,775$  GBq)/mg of Lu is possible in a several-day irradiation compared to the theoretical maximum of 110 Ci (4,070 GBq)/mg. The indirect route,  $^{176}\text{Yb}(\text{n}, \gamma)^{177}\text{Yb}$  ( $t_{1/2}$  1.9 h,  $\beta^-$ )  $\rightarrow$  Lu-177, has also been developed and presently the material is commercially available (MDS Nordion, Inc.). The advantage of this method is that it is a “no-carrier-added” route and contamination with Lu-177m is eliminated. With a 3.8b cross-section this reaction can yield reasonable quantities for research, but large-scale production for widespread clinical use is not likely. Also, because of the difficulty of cleanly separating rare earth elements it is not possible to remove all lanthanides from the product, so the effective specific activity is actually somewhat lower in this method than with direct production. High energy proton irradiation of natural Ta and Hf targets was very recently attempted at Brookhaven to make no-carrier-added Lutetium-177. However, the initial results were very disappointing, as the yield was very low and many other Lu isotopes are co-produced (Mausner and Mirzadeh 2003). At this time, using either of the reactor routes, Lu-177 is under active investigation by dozens of studies with radiolabeled peptides, e.g., SSTR positive lung tumors using Octreotate or DOTA-TOC, or antibodies, e.g., for prostate, ovarian cancer (CC49), lung (RS7), lymphoma (anti CD74), etc., as discussed elsewhere in detail in subsequent chapter(s) in this volume. Lutetium-177 is also utilized in radioimmunotherapy when chelated with tumor-associated antibodies and has also been proposed as a radioisotope source for

brachytherapy. Lutetium-177 g decays with a half-life of 6.7 d with gamma rays of 113 keV (6.6 %) and 208 keV (12 %) suitable for deep-organ imaging. The average  $\beta$  energy of Lu-177 g is 0.133 MeV and the average equilibrium dose rate constant for Lu-177 g is estimated to be  $\sim 0.5$  g-rad/ $\mu$ Ci-h (Mausner and Mirzadeh 2003).

The rather longer half-life of Lu-177 is better suited for slow-targeting antibodies, and its lower equilibrium dose rate constant makes Lu-177 useful for radiotherapy of soft tissues. In addition, Lu-177 has chemical characteristics suitable for protein labeling with bifunctional chelating agents such as the eight coordinated DTPA, DTPA derivatives, or DOTA. Although Lu is the heaviest member of the lanthanides, the ionic radius of Lu<sup>3+</sup> is expected to be comparable to that of Y<sup>3+</sup> as the result of lanthanide contraction. In coordination number 6, the ionic radius of Lu<sup>3+</sup> is 89.1 pm,  $\sim 4$  pm smaller than that of Y<sup>3+</sup>. At 25 °C and 0.1 M ionic strength, the equilibrium constant of Lu-DTPA complex (ML/M.L) is  $2.51 \times 10^{22} \text{ M}^{-1}$  in comparison with  $1.12 \times 10^{22} \text{ M}^{-1}$  for the Y-DTPA complex (Martell and Smith 1974).

Due to rather large cross-sections, high specific activity Lu-177 g can be obtained directly by Lu-<sup>176</sup>Lu[n, $\gamma$ ] reaction (Table 5). The natural abundance of Lu-176 g is, however, only 2.6 %. The highest Lu-176 enrichment readily available in the United States is 73 %. Alternatively, Lu-177 g can be obtained indirectly from beta decay of Yb-176 ( $t_{1/2} = 1.9$  h,  $E_B^{\text{max}} = 400$  keV), (Table 5). In this case, the Yb-176 parent nuclide is produced in a fission nuclear reactor with neutron capture on Yb-175 which has a natural abundance of 12.7 %. Enriched Yb-175 up to 96 % is also available in the United States. It is clear that the indirect route yields higher specific activity preparations of Lu-177, if Lu can be separated efficiently from Yb target material. A similar separation, for carrier-free Ho-166 from small quantities of Dy, was discussed in the preceding section. In addition, the indirect route produces Lu-177, which is free from 160-d Lu-177m. This impurity is unavoidably co-produced with Lu-177 by the <sup>176</sup>Lu9n, $\gamma$ 0 reaction (Mausner and Mirzadeh 2003).

For a 1-hour irradiation of two natural Lu targets, 4.8 and 9.1 mg as Lu<sub>2</sub>O<sub>3</sub>, at the position 4 of the HFIR hydraulic tube, the experimental yield of Lu-177 was 66 mCi/mg of Lu, corresponding to a value of 2.5 Ci/mg of Lu-176. The ratio of the Lu-177 m/Lu-177 g in this case is  $4.8 \times 10^{-3}\%$ . Under similar conditions, the yield from 43 % enriched Lu-176 targets (0.5–0.7 mg) were 1.1 Ci/mg of Lu and 2.6 Ci/mg of Lu-176 with a Lu-177m/Lu-177 g ratio of  $4.6 \times 10^{-3}\%$ . These data indicate that a yield of  $\sim 80$  Ci per mg of Lu-176 can be expected within 4 days in the position 4 of the hydraulic tube at ORNL. Obviously, the Lu-177 m/Lu-177 g ratio will increase with the irradiation time. For a 4-day irradiation the fraction of Lu-177 m

at EOB is expected to be less than 0.01 %. The yield of Lu-177 g from the indirect route (from decay of Yb-177) is 2.0 mCi/mg of Yb-176 for 1-h irradiation at the 5 position of the hydraulic tube. Although the yield from indirect route is lower than the direct route by a factor of 1,000, the specific activity of the Lu-177 from both routes will be almost the same assuming carrier-free Lu can be separated from Yb in 1 part per thousand (Mausner and Mirzadeh 2003).

### 7.1.6 Tungsten-188 and the Tungsten-188/Rhenium-188 Generator System

Recently, there has been considerable interest in Re-188 for various medical applications (see chapter by Knapp, et al. 2012). Since this is the subject of a separate chapter in this volume, only certain production and purification aspects and nuclear/chemical characteristics will be briefly covered here.

The convenient 16.9 h half-life and 100 % beta emission with high end-point energies ( $E_B^{\text{av}} = 764$  keV) make Re-188 an attractive candidate for radiotherapy of larger tumors. Rhenium-188 provides an ideal  $\gamma$ -ray at 155 keV for imaging with an intensity of 15 %. About 5 % of this transition also converts at the electronic shell of the Os providing low range secondary electrons and X-rays. The average equilibrium dose rate constant for Re-188 is 1.78 g-rad/ $\mu$ Ci-h. Another major advantage is the availability of Re-188 in the carrier-free state from a generator system with a shelf life of many months. The element Re is placed in Group VIIb of the periodic table under Mn and Technetium. These three elements have numerous valence states and complex electrochemistry. Similar to Tc, the most stable oxidation state of Re is +7 perrhenate (ReO<sub>4</sub><sup>-</sup>). In most complexes with ligands, however, Re assumes oxidation states of 4 or 5. Although there is some chemical resemblance of Re to that of Tc, there are significant chemical differences as well (Mausner and Mirzadeh 2003).

The parent nuclide, W-188, is produced in a nuclear reactor with double neutron capture on highly enriched W-186. The thin-target production yield of W-188 as a function of irradiation time at a neutron flux of  $2 \times 10^{15} \text{ ns}^{-1}\text{cm}^{-2}$  (HFIR) has been described (Mirzadeh et al. 1997a). The cross-section for the production of W-187, the intermediate radionuclide, is 37.9 b (Mughabgab et al. 1984). The thermal neutron cross-section for <sup>187</sup>W (n,  $\gamma$ )<sup>188</sup>W reaction is 14.5 b. The chemical form of the target can be either metallic or oxide. The main advantage of a metal target is a net increase in the yield per unit target, as a larger amount of W metal can be packed into an irradiation capsule. This is an important factor for the large scale production of W-188. The chemical processing of the neutron irradiated WO<sub>3</sub> targets involves dissolution in excess of hot 1 M NaOH in the presence of H<sub>2</sub>O<sub>2</sub> or NaOCl

or both (Knapp et al. 1994). One approach to process metallic W is to take advantage of the reactivity of molecular oxygen toward metallic W powder at elevated temperatures, and subsequent dissolution of the  $\text{WO}_3$  as above. This approach has an additional benefit in that the technique can be used for simultaneous separation of W from Re and Os which form volatile oxides (Mirzadeh et al. 2000).

Because of the chemical similarity to the Mo-99/Tc-99m pair, most efforts have focused on alumina-based generator systems where tungsten is retained on alumina in the form of tungsten oxide, tungstic acid, tungstates, isopolytungstates or phosphotungstates, and Re-188 (formed from the beta decay of W-188) is eluted with NaCl solutions (Callahan et al. 1989; Griffiths et al. 1984; Botros et al. 1986). Sorption of W-containing species was studied under various conditions including concentration and chemical form of tungsten, pH and anionic nature as well as solvent quality, and the treatment and granularity of the alumina support (Botros et al. 1986; Kadina et al. 1990). Alternatively, in a "Gel-Type" system W-188 is co-precipitated with zirconium hydroxide to form a gel, which is then packed in a column, and Re-188 is eluted with normal saline (Ehrhardt et al. 1987, 1990, 1992). Other systems developed over the years include zirconium oxide column (Lewis and Eldridge 1966; Balchot et al. 1969), tungsten fluoride absorbed on Dowex 1 anion exchanger in the fluoride form (Kamioki et al. 1994), and phosphotungstate on alumina (Mikheev et al. 1972).

The adsorption functions of  $\text{WO}_4^{2-}$  and  $\text{ReO}_4^-$  on alumina from  $\text{HNO}_3$ ,  $\text{HCl}$ , and  $\text{NaCl}$  data indicate that the highest distribution constant ( $K_d$ ) of  $10^4$  for  $\text{WO}_4^{2-}$  is obtained in 0.21 M NaCl, yet in the same solution the  $K_d$  of  $\text{ReO}_4^-$  is only 1.3 (Botros et al. 1986). An alumina-based W-188/Re-188 generator was evaluated for Re-188 yield and elution profile and W-188 breakthrough using various reagents for a 3-month period (Kamioki et al. 1994). The optimum concentration of cations for sharp elution of Re-188 is  $\sim 0.05$  M. Concentrations below this optimal value resulted in an increase in retention time as well as an increase in the full width half maximum (FWHM) of elution curve. While  $\text{NH}_4^+$  and  $\text{Na}^+$  ions had similar effects on the Re-188 elution behavior, the  $\text{NH}_4^+$  ions were found to be more effective than  $\text{H}^+$  ions of equal concentration. The yield of Re-188 from the generator displayed a gradual decrease, from 80 to 64 %, during the 3-month evaluation period. The breakthrough of W-188 per elution was as high as  $1.2 \times 10^{-2}$  % but decreased rapidly to  $3.2 \times 10^{-4}$  % within the first five elutions. In parallel studies, the adsorption dynamics of tungsten on alumina showed a sharp rise in the tungsten breakthrough at a  $\text{W}/\text{Al}_2\text{O}_3$  ratio of  $\sim 120$  mg/g, corresponding to a  $K_d$  of  $8.4 \times 10^3$  from nitrate solution at 0.05 M ionic strength (Dadachova and

Lambrech RM 1995). In continued studies, the surface interaction between  $\text{WO}_4^{2-}$  ions and the alumina support in the W-188/Re-188/ $\text{Al}_2\text{O}_3$  biomedical generator system was examined by the dynamic adsorption method, which employs the W-187 tracer, and by FT-IR, Raman, Al-27 MAS-NMR, and XPS spectroscopic methods. These studies demonstrated the complex physical and chemical nature of  $\text{WO}_4^{2-}$  ion adsorption on alumina. The dynamic adsorption studies indicated that the adsorption process includes several stages, from initial monolayer formation to almost complete saturation of the alumina surface. FTIR, Raman, and Al-27 MAS-NMR data showed that adsorption of  $\text{WO}_4^{2-}$  on the  $\text{Al}_2\text{O}_3$  surface in slightly acidic solutions proceeds via formation of thermodynamically stable complexes of tetrahedrally coordinated aluminum atoms and  $\text{WO}_4^{2-}$  tetrahedrons. The conclusion on the nature of  $\text{WO}_4^{2-}$ - $\text{Al}_2\text{O}_3$  complex in aqueous solutions was further supported by the results from XPS studies, where it was shown that W-containing species are strongly attached to the surface of alumina via W-O bonds (Dadachova and Lambrecht RM 1995).

The required volume for quantitative elution of Re-188 from a generator obviously depends on the size of the column which in turn is inversely proportional to the specific activity of W-188. The production of high specific activity W-188, however, is limited to only a few research nuclear reactors worldwide which have neutron fluxes of greater than  $10^{15}$  n.s $^{-1}$ .cm $^{-2}$ . To make use of low specific activity W-188 that can be produced in nuclear reactors with lower neutron fluxes, tandem alumina/anion-exchange generator systems have been proposed. In one approach, the proposed system was based on the observation that carrier-free Re-188 was strongly retained in a small anion exchange column from dilute  $\text{HNO}_3$  and then eluted with strong  $\text{HNO}_3$  in a small volume (Kamioki et al. 1994).

## 7.2 Alpha, Auger, and Conversion Electron Emitters

### 7.2.1 Alpha Emitters

As mentioned earlier, targeted alpha radiation therapy can be a very potent treatment of cancer (Dadachova 2010). Due to comparatively short range of alpha particles in tissue and their high LET nature, radiation damage is mainly confined to targeted cells. The radiation burden to the surrounding healthy tissues is low when compared to beta emitters. By facilitating an efficient delivery of alpha-emitting isotope it is possible to achieve a very effective treatment regimen for the types of cancer where microscopic and small volume tumors are present. The effectiveness of alpha radioimmunotherapy has been confirmed in clinical and preclinical trials. (Jurcic et al. 2002; Miederer et al. 2008).

A number of alpha emitting radioisotopes have been proposed as possible candidates. Among those are At-211, Bi-212, Bi-213, Ac-225, Pb-212, Ra-223, Tb-149, and Fm-255. Some of them (Bi-212, Bi-213, Ac-225, Pb-212, Ra-223) are produced from reactor irradiations, incorporated on generators and subsequently eluted. However, most of the clinical studies have been inhibited by a very limited supply of alpha-emitting isotopes, especially those that have theragnostic properties, for example, astatine-211,  $^{213}\text{Bi}$ , radium-223 ( $^{223}\text{Ra}$ ) and  $^{225}\text{Ac}$ . Three of these ( $^{213}\text{Bi}$ ,  $^{225}\text{Ac}$ , and  $^{223}\text{Ra}$ ) are presently produced from reactor neutron irradiations, incorporated on generators and subsequently eluted. Their parent nuclides are often fissile materials and require special safeguard requirements due to non-proliferation concerns. On the other hand, production of At-211, Tb-149, and Fm-255 require alpha beam (At-211), 600 MeV protons (Tb-149), or neutron irradiation of Curium (Fm-255). Only a very few facilities in the world have such capabilities, and most of these because of their other primary missions are not generally available for isotope production (Srivastava 2012).

#### 7.2.1.1 Astatine-211

Astatine-211 ( $t_{1/2}$  7.2 h) decays through two paths, each emitting an alpha particle. The mean alpha energy is a potent 6.8 MeV. It is produced by the  $^{209}\text{Bi}(\alpha, 2n)$  reaction and typically separated from the target by dry distillation into a chloroform solution (Larsen et al. 1996; Zalutsky et al. 2001). A difficulty in this process is that the cyclotron energy must be carefully controlled to minimize the co-production of Astatine-210. This isotope ( $t_{1/2}$  8.1 h) decays to Po-210 ( $t_{1/2}$  138 days) which is an alpha particle emitting bone seeker in vivo and could cause considerable hematological toxicity. The half-life of At-211 is relatively long compared to the other alpha emitters thus allowing time for chemistry of labeling and use for molecular carriers with slower tumor uptake. However, it is more easily catabolized and shed after cell internalization of the labeled antibody/antigen complex than the metallic alpha emitters (Yao et al. 2001). The main problem that inhibits clinical trials with this isotope is the relatively low nuclear yield and very limited number of cyclotrons capable of producing Astatine-211. This situation may be somewhat improved in the coming years when the ARRONAX cyclotron in Nantes, France, as expected, goes into routine operations in early 2013 (Haddad et al. 2011).

#### 7.2.1.2 Actinium-225/Bismuth-213 System

Targeted alpha radiation therapy with alpha emitters Ac-225 and Bi-213, as is the case with astatine-211 (vide supra), is also a very promising treatment of cancer (Dadachova 2010). If selective efficient delivery of these alpha-emitting isotopes to tumor cells is achieved, they can

become very effective for the treatment of the types of cancer where microscopic and small volume tumors are present. The effectiveness of alpha radioimmunotherapy using these isotopes has already shown promise in pre-clinical and clinical trials (Jurcic et al. 2002; Miederer et al. 2008). The results of the only human clinical trial involving an alpha-emitting isotope have demonstrated feasibility and antileukemic effects of Bi-213-HuM195, a humanized anti-CD33 MAb, specifically designed to target myeloid leukemia cells. In this study, 78–93 % of the subjects showed reduction in circulating and bone marrow blasts (Larsen et al. 1996). A clinically approved Ac-225/Bi-213 generator capable of producing 25–100 mCi of Bi-213, suitable for antibody labeling, was developed (McDevitt et al. 1999) and continues to be improved upon. The antibodies and peptides labeled with the generated Bi-213 have successfully been used in numerous preclinical and clinical trials (Jurcic et al. 2002; Miederer et al. 2008; McDevitt et al. 1999; Norenberg et al. 2006). As mentioned above, most of the clinical studies have been inhibited by a very limited supply of these and other alpha-emitting isotopes, especially those that have theragnostic properties, for example, At-211, Bi-213, Ra-223 and Ac-225Ac.

The in vivo use of targeted NCA Ac-225, in its own right, has received a great deal of attention as well (Geerlings et al. 1993; Miederer et al. 2008). Because of its ability to produce 4 alpha-emitting daughters, its overall potency to destroy cells is higher. The isotope has been referred to as an in vivo alpha particle nanogenerator because its power proliferates beyond the size of the atom (Miederer et al. 2008). In addition, the applications of Ac-225 were further extended to encapsulation in liposomes (Sofou et al. 2007) and metallofullerenes (Akiyama et al. 2009). At the Memorial Sloan–Kettering Cancer Center, a clinical trial for radioimmunotherapy of acute myeloid leukemia with both Bi-213 and Ac-225 has recently been carried out (Jurcic et al. 2006). As mentioned earlier in the text, Ac-225 has been used for radioimmuno-therapy both as a potent alpha emitter attached to an antibody and as a generator for the daughter alpha emitter Bi-213 ( $t_{1/2} = 45.7$  min). The decay of Bi-213 is accompanied by emission of 440.45 keV ( $I = 25.9$  %) gamma photon, which allows SPECT imaging to study pre-therapy biodistribution, pharmacokinetics, and dosimetry of the labeled radiopharmaceuticals. The current availability of Ac-225 is very limited and insufficient to support ongoing and proposed clinical trials. Currently, there are two suppliers of Ac-225. One is the US Department of Energy's ORNL and the other is the Institute for Transuranium Elements in Karlsruhe, Germany. Both suppliers obtain thorium-229 from uranium-233 that was produced as part of US molten salt breeder reactor program. The current stock of purified Th-229 at ORNL is 150-mCi. In an 8-week period, about

100 mCi of Ac-225 grows in from that supply, separated, and provided for clinical trials. Because Th-229 decays to Ac-225 through intermediate daughter Ra-225, Ra can be isolated to provide additional quantities (up to 20 mCi) of Ac-225 (Boll et al. 2005; Apostolidis et al. 2005; Zhuikov et al. 2011). Similarly, the Institute of Transuranium Elements can separate 43.2 mCi of Ra-225 and 39.4 mCi of Ac-225 from their stock (Apostolidis et al. 2005). It is widely acknowledged that the anticipated growth in demand for Ac-225 will soon exceed the levels extractable from the available uranium-233 (Boll et al. 2005).

At BNL, our intent is to carry out future investigations in an effort to increase the supply of Ac-225. This would involve using the high-energy proton spallation reaction  $^{232}\text{Th}(p,2p6n)^{225}\text{Ac}$  on natural Thorium. This method has recently been studied and developed at other places, in particular, at the Institute of Nuclear Research (INR) in Troitsk, Russia, using accelerated protons at energies between 90 and 145 MeV in their 160-MeV proton accelerator (Zhuikov et al. 2011). This investigation has pointed out that the yield of Ac-225 increases monotonically with the proton energy. Therefore, the BLIP at BNL (200 MeV) would be capable of producing almost twice as much with an incident energy on the target of 192 MeV, with 110- $\mu\text{A}$  beam intensity. The expected outcome of the BNL effort would be the method for Ac-225 production with quality (radionuclidic and chemical purity) suitable for applications both as a radiotherapeutic agent (Ac-225) and as a generator of Bi-213 (theragnostic use). The proposed work will involve development of an optimized Th-232 target for irradiation, development of the chemical procedure for dissolution and processing of irradiated target to selectively separate Ac-225, and carrying out preliminary labeling studies of conventional targeting molecules with Ac-225/Bi-213 to demonstrate the efficacy of the final purified radioisotope(s) for the eventual protein/antibody labeling applications.

At BNL, the method could potentially yield Curie amounts of Ac-225Ac in a 10-day irradiation period at the BLIP. The produced Ac-225 can be used for radioimmunotherapy as well as for generation of Bi-213 in a quality suitable for clinical trials. Shorter lived radioisotopes Ac-228,226,224 will be co-produced in quantities comparable with those of Ac-225, but the activities of these isotopes will saturate out during the 10-day irradiation. The radionuclidic purity of the Ac-225 can be improved by allowing a cool-off period for the target. Ten days (one  $t_{1/2}$  of Ac-225) after EOB, the co-produced Ac radionuclides will comprise 1 % of the activity of Ac-225. Among these, Ac-227, because of its 21.77-year half-life, is the only radioimpurity that might be of some concern as far as noninvasive imaging is concerned but, in principle, of less concern for theragnostic use.

However, this issue would require further investigation and additional studies.

Small quantities of Ac-225 can also be prepared by the reaction  $^{226}\text{Ra}(p,2n)^{225}\text{Ac}$  over an energy range of 13–20 MeV (Melville and Allen 2009). The cross section for this reaction is calculated to reach a peak of 700 mb at 16 MeV, but total yield is limited by the small energy range (and target thickness) where this reaction is favorable. Similarly, the photonuclear reaction  $^{226}\text{Ra}(\gamma,n)^{225}\text{Ra}$  ( $t_{1/2} = 14.9\text{d}$ ) followed by beta decay to Ac-225 is feasible but requires an extremely large Ra target ( $\sim 40\text{ g}$ ) that represents radiological safety issues and availability concerns.

Thus, Ac-225, when produced by the BNL method, could substantially add to the very limited present supply of this promising alpha emitter. According to experimental and theoretical extrapolations, and assuming certain target dimensions, radiochemical processing losses, and so forth, the projected yields from a 10-day irradiation at the 5 high-energy accelerators in the world are estimated (from the studies at INR) to be as follows (in Curies; experimental, and theoretical values within parentheses): BLIP at BNL, 3.1 (4.9); INR in Russia, 2.6 (4.1); IPF at LANL, 0.7 (1.3); Tri-University Meson Facility (TRIUMF) in Canada, 0.5 (0.7); and Arronax in France, 0.2 (0.7), giving a total of  $\sim 7$  (11) curies (Zhuikov et al. 2011). This would allow detailed preclinical and clinical studies to determine the therapeutic potential of Ac-225 itself as well as of the theragnostic daughter Bi-213. Many of the presently available bifunctional chelating agents as well as those based on cyclohexylethylenediamine tetraacetic acid (CDTA) and 1,4,7,10-tetraazacyclodecane-1,4,7,10-tetraacetic acid (DOTA) derivatives, developed earlier at BNL (Mease et al. 1997; Sweet et al. 2000), should allow linking Ac-225 and Bi-213 with protein-bifunctional chelating agent conjugates that will have high in vivo thermodynamic and kinetic stability. It would, of course, serve as a generator of Bi-213 similar to Ac-225, produced by the decay from Th-229.

## 7.2.2 Auger and Conversion Electron Emitters

The production of metastable nuclei such as conversion electron emitter Sn-117m and Auger electron emitter Pt-195m via neutron radiative capture reactions is characterized by small neutron cross-sections and, hence, low production rates. Metastable nuclei typically have excitation energies of the order of 100 keV, and large differences in angular momentum from ground states (most metastable nuclei have high angular momentum). An alternative route for producing these types of metastable nuclei is through neutron inelastic scattering where the cross-section of the  $^A\text{Z}(n, n')^{A\text{m}}\text{Z}$  reaction is, in some cases, substantially higher than the cross-section for the  $^{(A-1)}\text{Z}(n, \gamma)^{A\text{m}}\text{Z}$  route. As has been shown for the case of Sn-117m (Mausner et al. 1985), the magnitude of gain in the cross-section may compensate

**Table 10** Metastatic bone pain relief from Tin-117m DTPA: Phase II clinical studies<sup>a</sup>

Dose group (MBq/kg)	n <sup>b</sup>	Complete (100 %)	Patients experiencing relief		Total response (%)
			Partial (>50 %)	None (0–50 %)	
2.6	5	0	3	2	3 (60)
5.3	9	3	4	2	7 (78)
6.6	5	3	1	1	4 (80)
8.5	9	2	4	3	6 (67)
10.6	12	4	6	2	10 (83)
All Doses	40	12	18	10	30 (75)

<sup>a</sup> Total patients 57; 54 received a single dose and 3 received two doses each

<sup>b</sup> A total of 40 therapeutic administrations were assessable

for the relatively lower fast neutron flux from a well-moderated fission spectrum. Note that the excitation energy of metastable nuclei will represent the threshold for inelastic scattering. Large research reactors, such as HFIR at ORNL, and HFBR (now closed down) in the U.S., and at the Research Institute of Atomic Reactors (RIAR) in Dimitrovgrad, Russia, with significant epithermal and fast neutron fluxes, have been well suited for these types of reactions.

A systematic study of the production of Sn-117m, and Pt-195m in the hydraulic tube facility of the HFIR was reported (Mirzadeh et al. 1997b). In all three cases, the yields from the  $[n,n']$  reactions were higher than those obtained from the  $[n,\gamma]$  reactions. The relative gains in the specific activity of the unfiltered (no Cd filter) targets were 1.4, for Pt-195m, and 3.3 for Sn-117m. The excitation energies for Sn-117m and Pt-195m are 314.6 and 259.2 keV, respectively. Since the thresholds for these inelastic scattering reactions are well above the cadmium cutoff, Cd filters did not have any effect on the yield of these reactions. The corresponding cross-sections for the inelastic neutron scattering reactions for the production of Sn-117m, and Pt-195m are  $222 \pm 16$ , and  $287 \pm 20$  mb, respectively. A value of  $176 \pm 14$  mb for the cross-section of Sn-117  $[n, n']$  Sn-117m reaction obtained at HFBR was reported earlier (Mausner et al. 1985).

### 7.2.2.1 Conversion Electron Emitter Tin-117m

The most common method for Sn-117m production is based on irradiation of tin with neutrons using the  $^{117}\text{Sn}(n, n')^{117\text{m}}\text{Sn}$  reaction (Mausner et al. 1985). However, since this reactor production method is based on the inelastic neutron scattering reaction using enriched Sn-117 as a target, it results in Sn-117m with a low specific activity of about  $\leq 20$  Ci/g (Srivastava et al. 2004). Stannic complexes with Sn-117m of such specific activity, particularly Sn-117m<sup>4+</sup>-DTPA, effectively reduce pain from bone metastases without adverse reactions related to bone marrow, as demonstrated by the results presented in Tables 10

and 11 (Srivastava et al. 1998). However, such low specific activity does not allow scaling up the therapeutic doses for treating bone metastases. Also, it is not acceptable for radioimmunotherapy and for many other applications.

Although it is not possible to achieve a higher than about 22 mCi/mg of specific activity in the reactor-produced tin-117m (Srivastava et al. 2004), no-carrier-added tin-117m can be produced by proton irradiation of antimony via nuclear reactions  $(p, 2p3n)$  or  $(p, 2p5n)$  in an accelerator (Mausner et al. 1985; Ermolaev et al. 2009).

NCA Sn-117m can also be produced in an accelerator via a large number of other nuclear reactions. Using the  $^{115\text{m}}\text{In}(\alpha, pn)^{117\text{m}}\text{Sn}$  reaction over the energy range of 45–20 MeV, a relatively pure product is obtained; however, with very small yields (Qaim and Döhler 1984). In addition, the nuclear reaction  $^{116}\text{Cd}(\alpha, 3n)^{117\text{m}}\text{Sn}$  is also very useful for the production of NCA Sn-117m. The thick target yield over the energy range 47 → 20 MeV is about 150  $\mu\text{Ci}/\mu\text{Ah}$ . Unfortunately, the present limiting factor for the scaled-up production of Sn-117m via this route is the availability and power of existing alpha accelerators and targetry (Yamazaki and Ewan 1969). Using the BLIP at BNL, we have been producing NCA Sn-117m with the natural antimony  $^{(\text{natSb})}(\text{p}, xn)^{117\text{m}}\text{Sn}$  reaction over the energy range of 38–60 MeV for quite some time (Mausner et al. 1985). This process, with a cross section of 5 mb, was found enough to produce therapeutic quantities of Sn-117m with high specific activity. The specific activity when assumed to be wholly dependent on the amount of Sn impurity in the Sb target was calculated to be 30,000 mCi/mg for each part per million of Sn in the target. However, further theoretical cross-section calculations at the Institute of Nuclear Research (INR) in Troitsk, Russia (vide infra) have demonstrated that the proton energy range should be much broader, perhaps 40–130 MeV. The specific activity of Sn-117m depends mainly on the amount of stable tin, which is also generated during the irradiation of natural Sb, and the specific activity can vary from  $\sim 1,000$

**Table 11** Myelotoxicity levels<sup>a</sup> of radiopharmaceuticals for bone pain palliation

Radiopharmaceutical	Dose group (mCi/kg)	n	No. of patients with Grade $\geq 2$ toxicity	
			WBC	Platelets
Sr-89 Cl <sub>2</sub>	0.154	67	25 (37%)	41 (61%)
	0.040	161	48 (37%) <sup>b</sup>	
Re-186-HEDP	0.500–1.143	12	2 (17%)	3 (25%)
Sm-153-EDTMP	1.00	20	3 (15%)	5 (25%)
	1.50	4	3 (75%)	1 (25%)
	3.00	6	4 (100%)	2 (50%)
Sn-117m DTPA	0.143	9	1 (11%)	0 (0%)
	0.179	5	0 (0%)	0 (0%)
	0.286	12	1 (8%)	0 (0%)

<sup>a</sup> Using NCI criteria<sup>b</sup> Only hematological toxicity@ Grade  $\geq 2$  mentioned

to 3,000 mCi/mg at EOB, a range that is quite suitable for radiolabeling molecules that bind to saturable *in vivo* receptors.

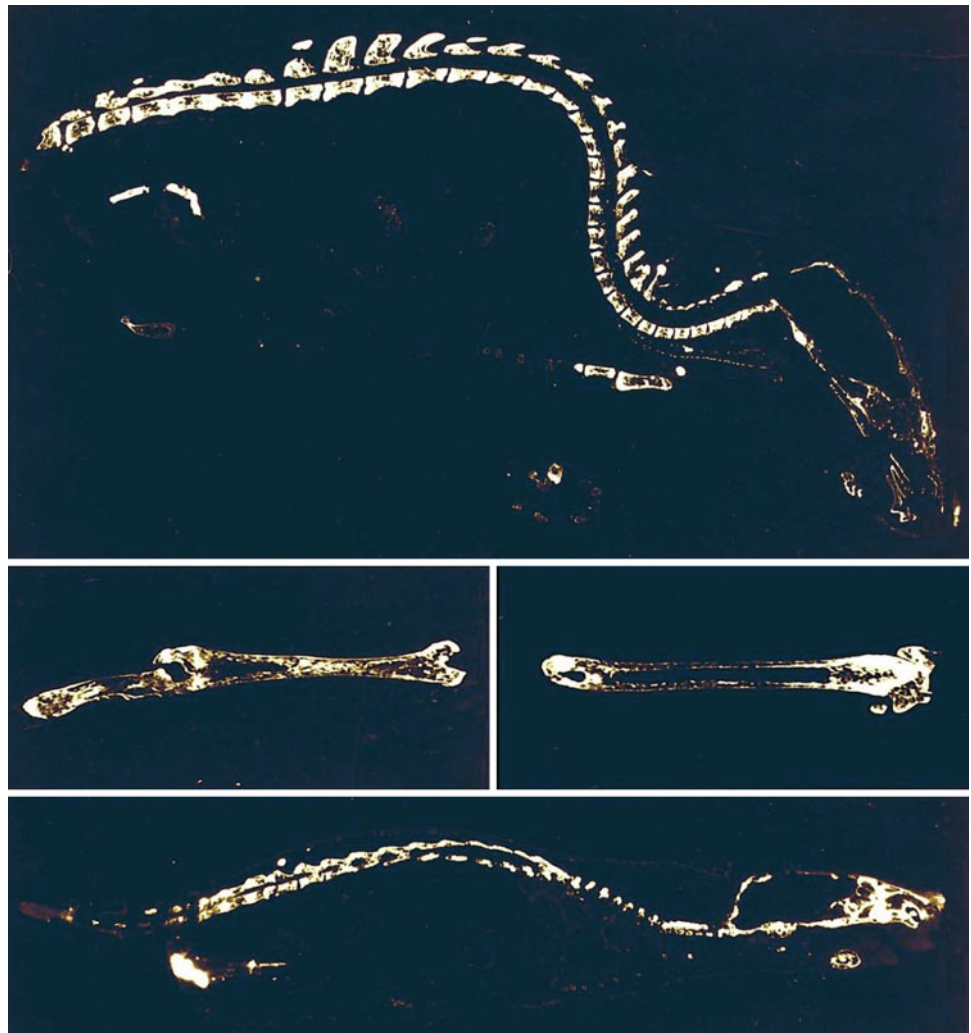
More recently, the larger scale accelerator production and availability of NCA Sn-117m with high purity and high specific activity, targets based on natural or enriched Sb have been developed in our collaborative research between BNL and INR, along with other institutes, including the Institute for Physics and Power Engineering in Obninsk (IPPE) and Moscow State University, in the neighboring regions in Russia (Ermolaev et al. 2009). This project was initiated under a US Department of Energy/National Nuclear Security Administration/Global Initiative for Proliferation Prevention (DOE/NNSA GIPP) Program in 1999 and completed in 2009. Results from this 10-year BNL/INR collaborative study have demonstrated and fulfilled the promise for the high-energy accelerator production of NCA Sn-117m in multi-Curie amounts for clinical theragnostic applications (Ermolaev et al. 2009).

Within this collaborative research program with BNL, investigations at INR dealt with the development of antimony as well as antimony/titanium intermetallic targets suitable for the high-energy production of NCA tin-117m. For irradiation with the high-intensity proton beam, targets consisting of Sb-monolith encapsulated into shells made of stainless steel or graphite were developed (Ermolaev et al. 2009). The shells were filled with metallic antimony as follows. Powdered metallic antimony was inserted into the shells under inert nitrogen atmosphere, and the filled shell was heated at 645–660 °C. It was found that at higher temperature liquid antimony reacts with iron and can destroy the stainless steel shell during the target preparation or irradiation. Graphite target shell is more reliable since there is no noticeable reaction between graphite and antimony, and graphite has higher heat conductivity than stainless steel [80–120 W/(m·K) vs. 20 W/(m·K) at

300 °C], providing effective target cooling. After antimony melting and shrinkage, the shell was again filled with powder of antimony and heated to melt again. The target with metallic shell containing a monolith of 29 g metallic antimony (a cylinder 9 mm thick, 30 mm in diameter) was hermetically sealed with a threaded plug. The graphite shell targets (plates 32 × 76 × 5 mm, 3 mm of Sb thick each, 19 g Sb each) were hermetically sealed with a cover by means of high temperature radiation resistant glue and electroplated outside with nickel in order to protect graphite from reaction with water radiolysis products during irradiation (Ermolaev et al. 2009).

The irradiated Sb-targets were chemically processed at the hot cell facility at IPPE in Obninsk. The stainless steel shell was dissolved in concentrated HCl while the graphite shell was opened mechanically. The freed Sb monolith was dissolved in concentrated HCl with gradual addition of small amount concentrated HNO<sub>3</sub>. The major amount of Sb (in the form Sb<sup>5+</sup>) was removed from the solution (10–11 M HCl) by extraction with dibutyl ether. Final purification of NCA Sn-117m from the rest of Sb, co-produced Te-118,119 m, 121 m, and In-111,114 m was achieved by chromatography on SiO<sub>2</sub> in 0.5 M sodium citrate (Na<sub>3</sub>Cit) solution. Tin isotopes remained adsorbed on SiO<sub>2</sub> while Sb and radioisotopes of Te and In were washed out. Then the column was washed with 0.5 M Na<sub>3</sub>Cit solution and water acidified by citric acid. Finally, tin was eluted from the column with 6 M HCl. Radionuclidic purity of the final solution and the specific activity of Sn-117m in the final product were determined using appropriate counting procedures (spectral emission analysis), and through ICP spectrometry. Among other isotopes of tin co-produced with Sn-117m, Sn-113 is the most important impurity. It has a long half-life (115 d), relatively high-energy  $\gamma$ -rays (392 keV) and cannot be chemically separated from Sn-117m. But it is possible to reduce Sn-113 impurity up to

**Fig. 5** Autoradiography in rats (*top*) and in mice (*middle* and *bottom*) demonstrates selective targeting and high uptake of tin-117m DTPA in bone and not in bone marrow or other organs (Swailem et al. 1998)



almost 1 % by lowering the initial proton energy. The optimum range of between 55 and 20 MeV has been demonstrated to be most effective, although at the expense of somewhat reduced Sn-117m product (Zhuikov et al. 2012).

Sn-117m ( $t_{1/2}$ , 14.0 days;  $\gamma$  159 keV, 86 %), as mentioned earlier in this chapter, is certainly one of the best radionuclides for the development of theragnostic radiopharmaceuticals, in particular, for nuclear oncology. In contrast to most other therapeutic beta emitters, Sn-117m decays via isomeric transition, with the emission of 3 major monoenergetic conversion electrons (127, 129, and 152 keV; abundance, 65, 12, and 26 %, respectively). These emissions with a very high LET have short discrete penetration ranges of between 0.22 (127 keV) and 0.29 mm (152 keV) in water. Therefore, Sn-117m when selectively targeted should be effective for therapy of metastatic disease and for certain other inflammatory conditions (e.g., atherosclerotic disease), causing much reduced myelosuppression and greatly reduced dose to normal organs [Howell

138]. This is schematically represented in Figs. 1 and 5, which show whole-body autoradiographies performed in mice and rats after the administration of Sn-117m( $4^+$ )-diethylenetriamine pentaacetic acid (DTPA), and the highly selective targeting and high uptake in bone by this agent, but not in bone marrow or other organs, suggesting the expected effectiveness of high-LET low-energy conversion electrons to produce intense radiation dose within a very short distance without affecting normal tissues, in particular, the radiation-sensitive bone marrow (Oster et al. 1985). Figure 6 shows whole body images in a prostate cancer patient, who had developed extensive bone metastases. The scan on the left was obtained using the standard Tc-99m MDP (methylene diphosphonate) imaging agent and the one on the right consists of scans obtained using tin-117m DTPA, an agent which as mentioned above has shown great promise for treatment of metastatic pain in prostate and breast cancer patients (Srivastava et al. 1998). These two scans are almost identical, demonstrating the specificity of tin-117m DTPA localization in bone and in much higher

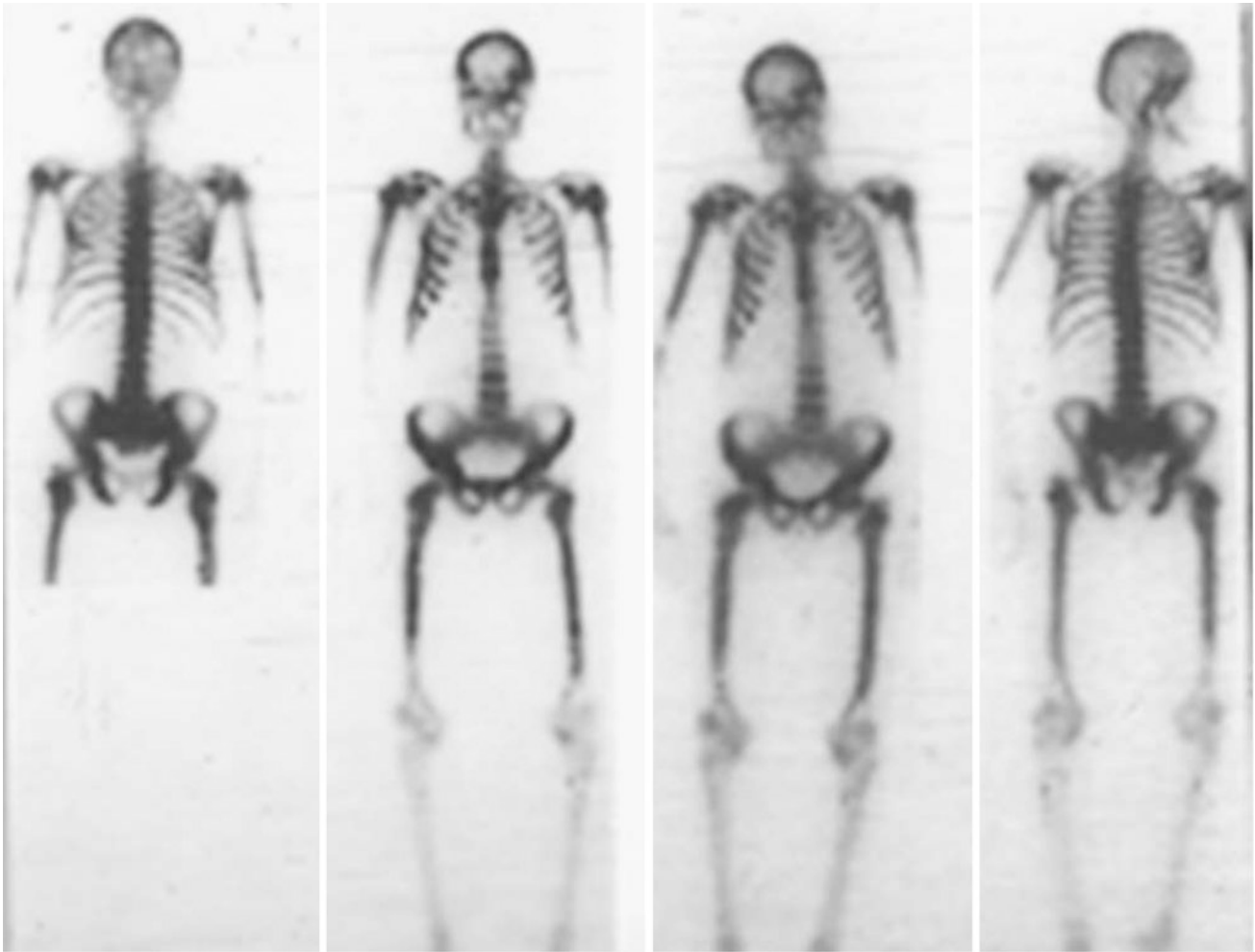


**Fig. 6** Whole-body images in a prostate cancer patient, who had developed extensive bone metastases. Scan on the *left* (posterior, anterior views) was obtained using the standard Tc-99m MDP bone imaging agent. On the *right* are scans (anterior, posterior)

obtained using tin-117m DTPA, which is promising for treatment of metastatic bone pain and potentially of osseous metastases (Srivastava et al. 1998)

concentration in bone metastases, in fact quantitatively even much better than the Tc-99m MDP. Figure 7, which is from an actual sample of bone tissue from a prostate cancer patient, who was treated with Sn-117m DTPA for bone pain palliation and who donated his body for research after death corroborates the same result as in Figs. 5 and 6. This latter patient had died of his primary cancer 47 days after therapy with 18.6 mCi (688 MBq) of Sn-117m DTPA, and the autopsy was carried out 6 h after death (Swailem et al. 1998). Figure 8 displays both a picture and the bone scintigraph of three longitudinal coronal slices (5 mm thick) of thoraco-lumbar vertebrae, again from the same patient as in Fig. 7. The uptake of Sn-117m DTPA is both diffuse (T8) and heterogeneous (L1). Partial involvement within a single vertebra indicates non-uniform distribution of radioactivity within the lesion, suggesting heterogeneous distribution of

metastatic foci (Swailem et al. 1998). Thus, the unique therapeutic emissions of Sn-117m also imply that their therapeutic effectiveness will be highly localized and should be lesion-specific and thus more effective. The use of Sn-117m DTPA is also very worth considering for an early stage disease at which time, there would be the possibility of slowing or even stopping the progression of further metastatic lesions. Moreover, having the 159-keV  $\gamma$  photon (86 %), which is very similar to that of technetium-99m, Sn-117m is perfect for pre-therapy imaging for dosimetry and for other information in the same patient as well as for monitoring the results of treatment (Swailem et al. 1998). All clinical studies thus far for bone pain palliation using Sn-117m DTPA were carried out using reactor-produced Sn-117m, with a specific activity ranging between 8 and 20 Ci/g of Sn. More recently, several 50–150-mCi

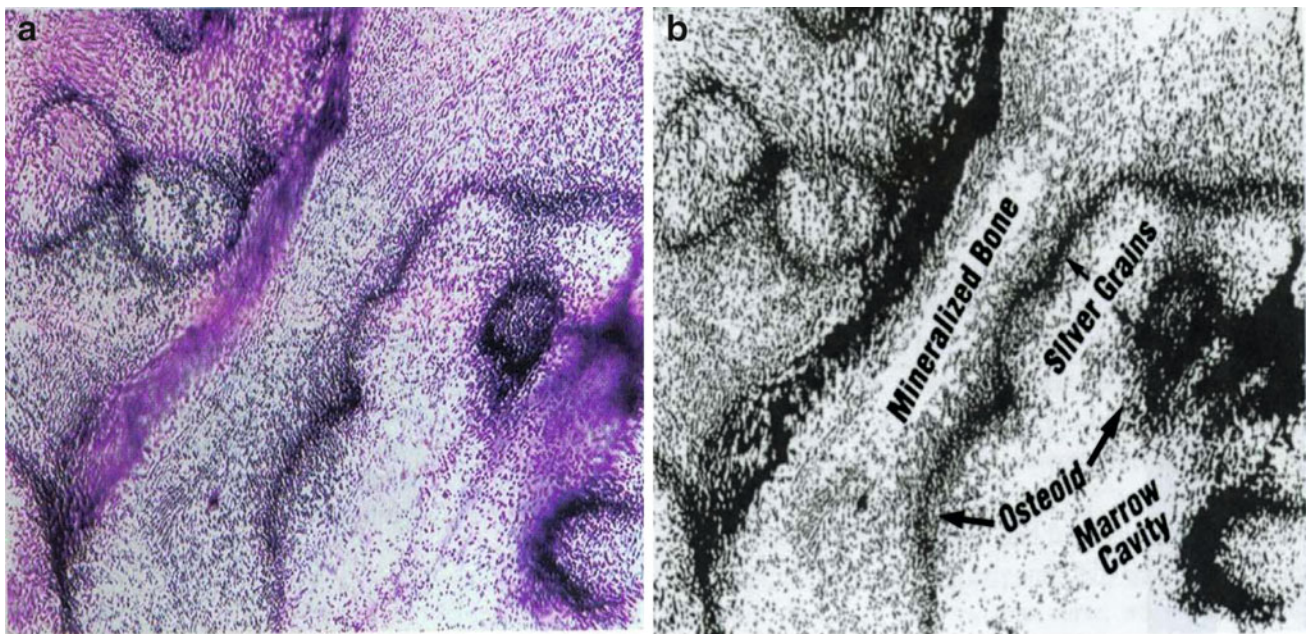
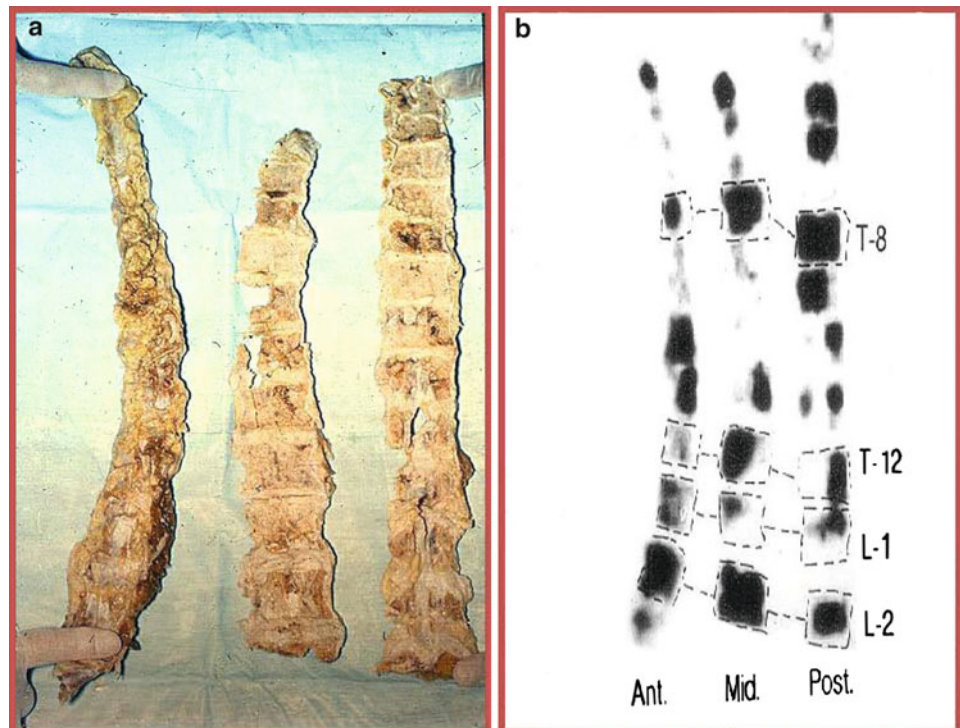


**Fig. 7** Microautoradiographic demonstration of the deposition of Sn-117m DTPA in bone (a) and a schematic diagram (b), showing sites of localization from a sample of bone obtained following the autopsy of a patient treated with Sn-117m DTPA for bone pain palliation. There is

high deposition in the actively mineralizing osteoid interface. Completely mineralized bone and the bone marrow space show very low deposition. Osteoid-to-marrow ratio is 11:1 (Li et al. 2007)

**Fig. 8** Photographic picture (a) and bone scintigraph (b) of three coronal slices (each 5 mm thick) of thoraco-lumbar vertebrae from the same patient as in Fig. 4. Partial involvement within a single vertebra indicates nonuniform distribution of radioactivity within the lesion, suggesting heterogeneous distribution of metastatic foci. Note the uptake in diseased areas in various sections according to the range of the Sn-117m conversion electrons (Li et al. 2007)



samples of NCA Sn-117m produced at INR as well as at the University of Washington alpha cyclotron, have successfully been used and evaluated at BNL, and in collaboration with

the Saint Joseph's Translational Research Institute in Atlanta and at other institutions, for effectiveness for theragnostic applications in animal models (Li et al. 2007, 2008).

Tin-117m, in addition to being a good therapeutic agent for cancer, also shows promise for the noninvasive molecular imaging and treatment of active atheromatous disease [vulnerable plaque (VP), also known as thin-cap fibroatheroma (TCFA)] in the coronary arteries and other areas of vasculature through the use of (i) coronary stents electroplated with Sn-117m or (ii) specific Sn-117m-labeled molecules systemically targeted to VP components. In the United States, there are, on an average, about 875,000–1,000,000 new heart attacks every year, and these are caused by two different types of atherosclerotic disease: luminal calcified plaque and extraluminal active atheromatous disease leading to the formation of VP. The luminal calcified plaques are easily detected by existing diagnostics, and the patient has a number of treatment options. However, VP develops and models positively outside the arterial lumen and cannot be detected by non-invasive imaging techniques. Unfortunately, more than 60 % of all significant cardiac events, including sudden death, are caused by the rupture of these thin-cap fibroatheroma lesions. The properties of Sn-117m as applied to VP's are unique and significant. Sn-117m-labeled Annexin effectively targets and binds to macrophage cells undergoing apoptosis, which are present in abundance in VPs. In relatively low doses, this agent can image the plaque using traditional SPECT gamma cameras with technetium-99m collimators and imaging protocols. Because of the longer half-life of Sn-117m combined with pre-targeting techniques, gamma cameras can acquire images long after the nonspecifically bound tin-Annexin has cleared the blood pool, thus improving the image quality (Narula et al. 2012).

At therapeutic doses, the conversion electrons from Sn-117m has been shown to reduce inflammation and, thus, are ideal for treating VPs, as their range in tissue ( $\sim 300 \mu\text{m}$ ) is approximately the same as the VP thickness in human coronary arteries. A clinical trial with Sn-117m-Annexin, begun in 2010, is currently in progress. At present, the phase IIa study (15 subjects) involves human carotid endarterectomy patients who are dosed and imaged for VP, with histology as the comparison. Further clinical trials (phase IIb and phase III) are in the planning stage. In recent studies in an Apo-E mouse VP model, in doses that appear to be imaging doses, tin-117m-Annexin has demonstrated a significant anti-inflammatory therapeutic effect. The plaque composition showed significantly less expression of macrophages in the low, middle, and high dose treatment groups as compared to the control group. In contrast, smooth muscle cell expression was greater in the middle and high dose groups as compared to the control, and in the low dose group, the difference was statistically significant between the low versus middle and high dose groups. (Srivastava et al. 2012a).

Because inflammatory cells are more radiosensitive than other arterial wall cell types, the conversion electrons should exhibit a beneficial anti-inflammatory effect in diseased coronary arteries. Since 28 days, corresponding to 2 half-lives of Sn-117m, is believed to be roughly the optimum period for neoproliferative tissue suppression, including neointimal proliferation after angioplasty and other primary interventional treatments in the coronary arteries and other vasculature, radiotherapy with Sn-117m should provide highly effective treatment, with minimal collateral damage to adjacent, quiescent arterial wall cells because of its low-energy conversion electron emission and short penetration in tissue. Furthermore, such limited energy delivery from a radioactive stent implant may circumvent the problem of cellular overgrowth at the implant edges, known as the “candy wrapper” effect, which has been observed with previous forms of radioactive stents.

At BNL, a novel radioactive stent stably electroplated with Sn-117m was developed as a therapeutic tool for the treatment of atherosclerotic coronary arteries (Srivastava et al. 2012b). Effects on vessel wall inflammation from various doses of electroplated Sn-117m were studied in hyperlipidemic rabbits. Three days after stent implantation in the abdominal aorta (4 doses: 0- [cold tin], 30-, 60-, and 150- $\mu\text{Ci}$  Sn-117m per 15-mm stent), the rabbits were sacrificed. Immunohistochemical analysis of proliferating macrophages and smooth muscle cells demonstrated that inflammatory cells in the Sn-117m-stented segments were dramatically reduced in a dose-dependent manner (Li et al 2007, 2008). The anti-inflammatory therapeutic effectiveness of the tin-117m-stent implants was further demonstrated in a preliminary study in pigs (24 pigs, 72 bare metal stent implants: 0–400- $\mu\text{Ci}$  Sn-117m per 15-mm stent), which was carried out to investigate the effects on in-stent neointima formation. The electroplating process appeared benign because the response from “cold” tin-plated stents was indistinguishable from what was observed for routinely used bare metal, 316L surgical stainless steel stents. A profound and unique radiation effect was consistently observed in the higher dose implants, which consisted of a discrete zone of dense connective tissue consolidation in the tunica adventitia, of  $\sim 0.25$ - to  $0.30$ -mm thickness, corresponding to the anticipated tissue penetration of the Sn-117m conversion electron energy. Focal suppression of in-stent neointima formation was also observed, but further study will be needed to determine, with certainty, the therapeutic potential of Sn-117m-electroplated stents for prevention of in-stent restenosis (Li et al. 2012).

NCA Sn-117m is also being developed and tested for the therapy of bone metastases and for use in radioimmunotherapy. A phase I clinical trial for the imaging and treatment of bone metastases using Sn-117m DTPA in prostate cancer patients is in the planning stage for 2013.

**Table 12** Choice of radionuclides for principal therapeutic applications<sup>a</sup>

Application	Route of administration	Best-suited radionuclide(s)
I. Tumor therapy		
(i) Solid tumors		
a. Large lesions	i.v.	Sc-47, Y-90, I-131, Lu-177, Re-188
b. Micrometastases	Intra-tumoral i.v.	Sc-47, Sm-153, Re-188 Sc-47, Sn-117m, Sm-153, other Auger, conversion electron, alpha, and short-range $\beta^-$ emitters
(ii) Leukemias, lymphomas	i.v.	Sc-47, Cu-67, Sn-117m, I-131, alpha emitters
II. Pain palliation		
(i) Soft tissue	i.v.	Y-90, I-131, Ho-166, Re-188
(ii) Metastatic bone pain	i.v.	Sr-89, Sn-117m, Sm-153, Re-186, Re-188
III. Non-oncology		
(i) Synovectomy	Regional	Sc-47, Sn-117m, Sm-153, Er-69
(ii) Marrow ablation	i.v.	Sn-117m, Ho-166
(iii) Microspheres	i.v.	Y-90, other radio-lanthanides
IV. Receptor-binding tracers; cellular (intranuclear) antigens	i.v.	Auger, conversion electron, alpha, and short-range $\beta^-$ emitters

<sup>a</sup> The isotopes in various categories are listed in order of increasing atomic mass and not necessarily based on their degree of their therapeutic effectiveness

### 7.2.2.2 Auger Electron Emitters Platinum-195m and Mercury-195m

As stated earlier, Pt-195m delivers the most dose of low energy particles. It can be produced in a straightforward fashion by the  $^{194}\text{Pt}(n, \gamma)$  reaction. However, as is typical for high mass metastable nuclei, the excitation energy is high (259.2 keV) and there is a large difference in angular momentum from the ground state ( $13/2 +$  from  $1/2 -$ ). The thermal neutron cross-section is only 42mb and thus the yield and specific activity are quite low (Hoeschele et al. 1982). In addition, the burn-up cross-section of Pt-195 m is 13,000 barns (Bett et al. 1983). Other approaches have been tried to improve the yield and specific activity by using inelastic neutron scattering with epithermal and fast neutrons to exceed the threshold for the metastable state. The  $^{195}\text{Pt}(n, n')$  and  $^{196}\text{Pt}(n, 2n)$  reactions were investigated (Hoeschele et al. 1982). The effective cross-section using a Pt-195 target is much higher at 287mb, but lower neutron flux in the proper energy range results in only a factor of 1.4 increase in the specific activity compared to the simple Pt-194 neutron absorption route. The (n, 2n) reaction has only a very low 3.7mb cross-section. In addition, we have studied the charged particle reaction  $^{192}\text{Os}(\alpha, n)^{195}\text{Pt}$  at the old BNL cyclotron and measured only a 1.2mb cross-section from 44 to 31 MeV. In short, there is no practical way to make enough Pt-195 m with adequate specific activity for radioimmunotherapy.

This leaves only Hg-195 m to consider. It can be produced by the  $^{197}\text{Au}(p, 3n)$  reaction on gold foil. A production yield using 0.5 mm thick foils of metallic gold with

34 MeV protons gave a reasonable yield of 4.6 mCi ( $\sim 0.17$  GBq) per  $\mu\text{Ah}$  at the end of bombardment (Bett et al. 1983). Thus, a high current cyclotron can produce therapeutic quantities. The difficulty is that the previous use of this isotope was as the parent in the Hg-195m/Au-195 generator system and the Hg-195m was not produced in a no-carrier-added form. Carrier mercury was added in processing to improve radioactivity recovery. Given the neurotoxicity of mercury, very high specific activity will be critical for in vivo use. Thus, the development of a better chemical separation method could make this Auger emitter useable for radioimmunotherapy investigations.

## 8 Conclusion

There are a number of existing and potential future radionuclides for use as unsealed sources for targeted therapy of cancer and for other therapeutic applications in nuclear medicine. The various important therapeutic applications where radionuclide therapy would have an important role to play in, and the radionuclides best suited for that particular type of application, are summarized in Table 12. It should be noted that this listing is not meant to be exhaustive and additional radionuclides can be added based on present and future work as well as various other considerations.

Most of the therapeutic radionuclides that are described in this chapter are presently available or are under investigation and many of these, especially those in the latter category, may eventually turn out to be ideal or best suited

for specific applications. Accordingly, this chapter has attempted to provide a description of the methods of production, and physical, nuclear, and chemical characteristics of many of these radionuclides in relation to the various current and intended future applications. Although issues related to cost and availability of a number of “future” radionuclides are yet to be addressed to everybody’s satisfaction, there does not seem to be a dearth of new therapeutic radionuclides. As new needs and applications develop, appropriate radionuclides will follow. Unfortunately, the cost and the availability, especially if the radionuclide is “new” and/or difficult to produce in meaningful quantities at reasonable cost, will remain issues of paramount importance.

The substantial progress of investigations in areas such as the treatment of cancer as well as of other inflammatory conditions such as in bone pain palliation, radiosynovectomy, and of many other disorders that respond to radionuclide therapy, offers renewed hope and promise for the widespread use of internally administered radionuclides for a number of novel and effective therapeutic approaches. Therapeutic nuclear medicine finally seems to be destined to find its rightful place in the “personalized” therapy of patients with the use of a number of dual-purpose (“theragnostic”) radionuclides or radionuclide pairs that are also discussed in this chapter. This paradigm when properly enforced would constitute a major step forward to meet the challenges of enabling personalized medicine. Theragnostic radiopharmaceuticals have the power to drive advances in personalized medicine that will offer better-targeted diagnosis and treatments. Using this approach, it would be possible to envision a future where treatments are tailored to individual patients’ specific disease parameters and where imaging data could be analyzed in real-time and in advance to predict likely effectiveness of therapy and learn what would or would not work. Implementation of this regimen potentially creates a situation where treatments are better targeted, health systems save money by identifying therapies not likely to be effective for particular patients, and researchers have a better understanding of comparative effectiveness.

However, an increased and reliable availability at reasonable cost of some of the best theragnostic radionuclides has remained a major issue, which must be addressed before we can successfully put this paradigm into routine clinical practice. This issue has been discussed in this article in some detail, and the evolving new methodologies for the production of some very promising theragnostic radionuclides have also been covered. It is worth emphasizing that the nuclear medicine modality is the only modality that can fulfill the dream of carrying out tailored personalized medicine by way of enabling diagnosis followed by therapy in the same patient with the same radiopharmaceutical. This

would be an exciting development with a very promising future, would be of invaluable benefit to cancer patients, and may very well mark the future of the field of nuclear medicine.

**Acknowledgments** This work was supported by the United States Department of Energy, Office of Science/Office of Nuclear Physics/Isotope Development and Production for Research and Applications Program, and the NNSA-NA-24 GIPP Program, under Contract No. DE-AC02-98CH10886 at Brookhaven National Laboratory. Comprehensive discussions took place with Dr. Saed Mirzadeh (Oak Ridge National Laboratory) on reactor production and with Dr. David Schlyer (BNL) on accelerator production of radionuclides. Both of them provided very informative material, some of which is included in this chapter, and their help is gratefully acknowledged.

## References

- Adelstein SJ, Kassis AI (1987) Radiobiologic implications of the microscopic distribution of energy from radionuclides. *Nucl Med Biol* 14:165–169
- Akiyama K, Haba H, Tsukada K et al (2009) A metallofullerene that encapsulates Ac-225. *J. Radioanal Nucl Chem* 280:329
- Apostolidis C, Molinet R, Rasmussen G et al (2005) Production of Ac-225 from Th-229 for targeted alpha therapy. *Analytical Chem* 77:6288
- Aslam MN, Sudar S, Hussain M, Malik AA et al (2001) Evaluation of excitation functions of  $^3\text{He}$  and  $\alpha$ -particle induced reactions on antimony isotopes with special relevance to the production of iodine-124. *Appl Radiat Isot* 69:94–104
- Balchot J, Herment J, Moussa A (1969) Un Generateur de Re-188 a Partir de W-188. *Int J App Radiat Isot* 20:467–470
- Bett R, Cuninghame JG, Sims HE et al (1983) Development and use of the  $^{195}\text{Hg}$ - $^{195}\text{Au}$  generator for first pass radionuclide angiography of the heart. *Appl Radiat Isot* 34:959–963
- Bigler RE, Zanzanico PB (1988) Adjuvant radioimmunotherapy for micrometastases. In: Srivastava SC (ed) *Radiolabeled monoclonal antibodies for imaging and therapy*, Plenum, New York, pp 409–428
- Bohr N (1936) Neutron capture and nuclear constitution. *Nature* 137(3461):344–348
- Boll RA, Malkemus D, Mirzadeh S (2005) Production of actinium-225 for alpha particle mediated radioimmunotherapy. *Appl Radiat Isot* 62:667
- Botros N, El-Garhy M, Abdulla S, Aly HF (1986) Comparative studies on the development of W-188/Re-188 generator. *Isotopenpraxis* 22:368–371
- Bradley EW, Chan PC, Adelstein SJ (1975) The radiotoxicity of I-125 in mammalian cells. I. Effects on the survival curve of radioiodine incorporated into DNA. *Radiat Res* 64:555–563
- Britton KE, Mather SJ, Granowska M (1991) Radiolabelled monoclonal antibodies in oncology III. Radioimmunotherapy. *Nucl Med Commun* 12:333–347
- Brown LC (1971) Chemical processing of a cyclotron-produced  $^{67}\text{Ga}$ . *Int J Radiat Isot* 22:710–713
- Brown LC (1972) Cyclotron processing of carrier-free  $^{111}\text{In}$ . *Int J Appl Radiat Isot* 23:57–63
- Buchegger F, Vacca A, Carrel S et al (1988) Radioimmunotherapy of human colon carcinoma by I-131 labeled monoclonal antibodies in a mouse model. *Int J Cancer* 41:127–134
- Buick RN, Pullam R, Bizzari JB et al (1983) The phenotypic heterogeneity of human ovarian tumor cells in relation to cell

- function. In: Burchiel SW, Rhodes BA (eds) Radioimmunoimaging and radioimmunotherapy, Elsevier, New York, pp 3–10
- Callahan AP, Rice DE, Knapp FF Jr (1989) Rhenium-188 for therapeutic applications from an alumina-based Tungsten-188/Rhenium-188 radionuclide generator. *NucCompact* 20:3
- Carlsson J, Aronsson EF, Hoetala S, Stigbrand T, Tennvall J (2003) Tumor therapy with radionuclides: assessment of progress and problems. *Radiother Oncol* 66:107–117
- Chan PC, Lisco E, Lisco H et al (1976) The radiotoxicity of I-125 in mammalian cells. II. A comparative study on cell survival and cytotoxic responses to IUDR-125, and HTdR-3. *Radiat Res* 67:332–343
- Cohen BL (1977) High level radioactive waste from light water reactors. *Rev Mod Phys* 49:1–20
- Dadachova E (2010) Cancer therapy with alpha-emitters labeled peptides. *Semin Nucl Med* 40:204–208
- Dadachova E, Mirzadeh S, Lambrecht RM (1995) Tungstate-ion-alumina interaction in a 188W/188Re biomedical generator. *J Phys Chem* 99:10976–10981
- Dadachova E, Mirzadeh S, Lambrecht RM, Hetherington EL, Knapp FF Jr (1994) Separation of carrier-free holmium-166 from neutron-irradiated dysprosium targets. *J Anal Chem* 66:4272
- Dadachova E, Mirzadeh S, Lambrecht RM, Hetherington E, Knapp FF Jr (1995) Separation of carrier-free  $^{166}\text{Ho}$  from  $\text{Dy}_2\text{O}_3$  targets by partition chromatography and electrophoresis. *J Radioanal Nucl Chem—Lett* 199:115–123
- Dadachova E, Mirzadeh S, Smith SV, Knapp FF Jr, Hetherington EL (1997) Radiolabeling antibodies with Holmium-166. *Appl Radiat Isot* 48:477–481
- Dale RG (1985) The application of linear-quadratic dose-effect to fractionated and protracted radiotherapy. *Br J Radiol* 58:515–528
- Dasgupta AK, Mausner LF, Srivastava SC (1991) A new separation procedure for  $^{67}\text{Cu}$  from proton irradiation of Zn. *Int J Radiat Appl Instrum Part A Appl Radiat Isot* 42:371–376
- Deconinck G (1978) Introduction to radioanalytical physics, Nuclear methods monographs No. 1, Elsevier Scientific Publishing Co. Amsterdam
- DeNardo SJ, Erickson K, Benjamini E et al (1982) Monoclonal antibodies for radiation therapy of melanoma. In: Raynaud (ed) Nuclear medicine and biology, Pergamon, Paris, p 182
- DeNardo G, DeNardo SJ, Macey DJ (1988) Quantitative pharmacokinetics of radiolabeled monoclonal antibodies for imaging and therapy in patients. In: Srivastava SC (ed) Radiolabeled monoclonal antibodies for imaging and therapy, Plenum, New York, pp 293–310
- DeNardo GL, DeNardo SJ, Kukis DL, O'Donnell RT et al (1998) Maximum tolerated dose of  $^{67}\text{Cu}$ -2IT-BAT-LYM-1 for fractionated radioimmunotherapy of non-Hodgkin's lymphoma: a pilot study. *Anticancer Res* 18:2779–2788
- DeNardo SJ, DeNardo GL, Kukis DL et al (1999)  $^{67}\text{Cu}$ -2IT-BAT-Lym-1 pharmacokinetics, radiation dosimetry, toxicity and tumor regression in patients with lymphoma. *J Nucl Med* 40:302–310
- Ehrhardt G, Ketring AR, Turpin TA et al (1987) An improved tungsten-188/rhenium-188 generator for radiotherapeutic applications. *J Nucl Med* 28:656
- Ehrhardt GJ, Turpin TA, Razavi MS et al (1990) A convenient tungsten-188/rhenium-188 generator for radiotherapeutic applications using low specific activity Tungsten-188. In: Nicolini M, Bandoli G, Mazzi U (eds) Technetium and rhenium in chemistry and nuclear medicine, Raven Press, New York, p 631
- Ehrhardt GJ, Ketring AR, Liang Q (1992) Improved 188W/188Re zirconiumtungstate. Gel radioisotope generator chemistry. *Radioact Radiochem* 3:38–41
- Ermolaev SV, Zhukov BL, Kokhanyuk VM, Srivastava SC et al (2009) Production of no-carrier-added Tin-117m from proton irradiated antimony. *J Radioanal Chem* 280:319–324
- Evans CC, Stevenson J (1956) Improvements in or relating to production of radioactive Iodine -131, British Patent 763865
- Evans CC, Stevenson J (1957) Production of radioactive phosphorous. British Patent 765,489
- Fabre JW, Daar AS (1983) Expression of normal epithelial membrane antigens on human colorectal and breast carcinomas. In: Burchiel SW, Rhodes BA (eds) Radioimmunoimaging and radioimmunotherapy, Elsevier, New York, pp 143–157
- Feinendegen LE (1975) Biological damage from the Auger effect: possible benefits. *Radiat Environ Biophys* 12:85–99
- Fowler JF (1991) Radiobiological aspects of low dose rates in radioimmunotherapy. *Int J Radiat Oncol Biol Phys* 18:1261–1269
- Fritzberg AR, Berninger RW, Hadley SW, et al (1988) Approaches to labeling of antibodies for diagnosis and therapy of cancer. *Pharm Res* 5:325
- Gandarias-Cruz D, Okamoto K (1988) Status on the compilation of nuclear data for medical radioisotopes produced by accelerators, IAEA Report INDC(NDS)-209/GZ
- Gansow OA (1991) Newer approaches to the radiolabeling of monoclonal antibodies by use of metal chelates. *Nucl Med Biol* 18:369–381
- Geerlings MW, Kaspersen FM, Apostolidis C et al (1993) The feasibility of Ac-225 as a source of alpha-particles in radioimmunotherapy. *Nucl Med Commun* 14:121
- Glasstone S, Sesonske A (1963) Nuclear reactor engineering. Van Nostrand, Princeton
- Griffith MH, Yorke ED, Wessels BW et al (1988) Direct dose confirmation of quantitative autoradiography with micro-TLD measurements for radioimmunotherapy. *J Nucl Med* 29:1795–1809
- Griffiths GL, Goldenberg DM, Sharky RM, Knapp FF, Jr., Callahan AP, Tejada G, Hansen HJ (1984) Radionuclide generators. In: Knapp FF, Butler TA (eds) ACS advances in chemistry, Series No. 214, American Chemical Society, Washington, pp 33–37
- Guillaume M, Lambrecht RM, Wolf AP (1975) Cyclotron production of  $^{123}\text{Xe}$  and high purity  $^{123}\text{I}$ : a comparison of tellurium targets. *Int J Appl Radiat Isotopes* 26:703–707
- Haddad F, Barbet J, Chatal J-F (2011) The ARRONAX project. *Curr Radiopharm* 4:186–196
- Herzog H, Rösch F, Stöcklin G et al (1993) Measurement of pharmacokinetics of Yttrium-86 radiopharmaceuticals with PET and radiation dose calculation of analogous Yttrium-90 radiotherapeutics. *J Nucl Med* 34:2222–2236
- Hnatowich DJ (1990) Antibody radiolabeling, problems and promises. *Nucl Med Biol* 17:49–55
- Hoesechel JD, Butler T, Roberts J, Guyer C (1982) Analysis and refinement of the microspace synthesis of the  $^{195}\text{mPt}$ -labeled antitumor drug, cis-DDP. *Radiochim Acta* 31:27–36
- Huclier-Markai S, Sabatie A, Kubicek V et al (2011) Chemical and biological evaluation of scandium (III)-polyamino-polycarboxylate complexes as potential PET agent and radiopharmaceutical. *Radiochim Acta* 99:653–662
- Humm JL (1986) Dosimetric aspects of radiolabeled antibodies for tumor therapy. *J Nucl Med* 27:1490–1497
- Hupf HB (1976) Production and purification of radionuclides. In: Tubis M, Wolf A (eds) Radiopharmacy. Wiley, New York, pp 225–253
- Jungerman JA, Yu Kin-Hung P, Zanelli CI (1984) Radiation absorbed dose estimates at the cellular level for some electron emitting radionuclides for radioimmunotherapy. *Int J Appl Radiat Isot* 35:883–888
- Jurcic JG, Larson SM, Sgouros G et al (2002) Targeted particle immunotherapy for myeloid leukemia. *Blood* 100:1233
- Jurcic JG, McDevitt MR, Pandit-Taskar N et al (2006) Alpha-particle immunotherapy for acute myeloid leukemia (AML) with bismuth-213 and actinium-225. *Cancer Biother Radiopharm* 21:40
- Kadina G, Tulsakaya T, Gureev E, Brodskaya G, Gapurova O, and Drosdovsky B (1990) Production and investigation of the

- Rhenium-188 generator. In: Nicolini M, Bandoli G and Mazzi U (eds) *Technetium and rhenium in chemistry and nuclear medicine*, Raven Press, New York, p 6353
- Kamioki H, Mirzadeh S, Lambrecht RM, Knapp FF Jr, Dadachova E (1994) 188W/188Re Generator for biomedical applications. *Radiochim Acta* 65:39–46
- Kassis AI, Adelstein SJ, Haycock C et al (1982) Lethality of Auger electrons from the decay of Br-77 in the DNA of mammalian cells. *Radiat Res* 90:362–373
- Knapp FF Jr, Callahan AP, Beets AL, Mirzadeh S, Hsieh B-T (1994) Processing of reactor-produced Tungsten-188 for fabrication of clinical scale alumina-based Tungsten-188/Rhenium-188 generators. *Appl Radiat Isot* 45:1123–1128
- Knapp FF, Kropp J, Liepe K (2012) Rhenium-188 generator-based radiopharmaceuticals for therapy. In: *Medical Radiology. Radiation Oncology*, Springer-Verlag, Berlin
- Kolsky KL, Joshi V, Mausner LF, Srivastava SC (1998) Radiochemical purification of no-carrier-added Scandium-47 for radioimmunotherapy. *Appl Radiat Isot* 49:1541–1549
- Lagunas-Solar MC, Jungerman JA (1979) Cyclotron production of carrier-free cobalt-55, a new positron-emitting label for bleomycin. *Int J Radiat Isot* 30:25–32
- Lambrech RM, Wolf AP (1973) Cyclotron and short-lived halogen isotopes for radiopharmaceutical applications. In: *New developments in radiopharmaceuticals and labelled compounds*, vol 1, IAEA, Vienna, pp 275–290
- Larsen RH, Wieland BW, Zalustsky MR (1996) Evaluation of an internal cyclotron target for the production of At-211 via the Bi-209(alpha,n)At-211 reaction. *Appl Radiat Isot* 47:135–143
- Larson S, Carrasquillo J, Reynolds J et al (1988) The National Institutes of Health experience with radiolabeled monoclonal antibodies: lymphoma, melanoma, and colon cancer. In: Srivastava SC (ed) *Radiolabeled monoclonal antibodies for imaging and therapy*, Plenum, pp 393–407
- Lewis RE, Eldridge JS (1966) Production of 70-day tungsten-188 and development of a 17 hour rhenium-188 radioisotope generator. *J Nucl Med* 7:804
- Li J, Mueller DW, Srivastava SC et al: Intravascular Stents Electroplated with Sn-117m reduce arterial wall inflammation in hyperlipemic rabbits. Presented at the GLS 2007 Meeting, Oct 3, 2007, Atlanta (abstr)
- Li J, Mueller DW, Srivastava SC et al (2008) Intravascular stents electroplated with <sup>117m</sup>Sn reduce arterial wall inflammation in hyperlipidemic rabbits. Presented at the 2008 ACC Annual Meeting, Chicago, May, 2008 (abstr)
- Li J, Mueller DW, Srivastava SC, Gonzales G, Chronos N et al (2012) publication in progress
- Liverhaut SE (1960) *Elementary introduction to reactor physics*. Wiley Interscience, New York
- Mani RS, Majali AB (1966) Production of carrier free <sup>32</sup>P. *Indian J Chem* 4:391
- Martell AE, Smith RM (1974) *Critical stability constants*, vol 1, Amino acids, Plenum Press, New York
- Mausner LF (1999) Radiochemical laboratory. In: *McGraw Hill encyclopedia of science & technology*, 9th edn. McGraw Hill, New York
- Mausner LF, Mirzadeh S (2003) Reactor production of radionuclides. In: Welch MJ, Redvanly CS (eds) *Handbook of radiopharmaceuticals*, Wiley, Chichester
- Mausner LF, Srivastava SC (1993) Selection of radionuclides for radioimmunotherapy. *Med Phys* 20:503–509
- Mausner LF, Mirzadeh S, Ward TE (1985) Nuclear data for production of <sup>117m</sup>Sn for biomedical application. In: *Proceedings of the international conference on nuclear data for basic and applied science*, Santa Fe, New Mexico, May, pp 733–737
- Mausner LF, Mirzadeh S, Maher R et al (1989) Production of high specific activity <sup>117m</sup>Sn with the Szilard-Chalmers process. *J Labelled Comp Rad* 16:177–178
- Mausner LF, Mirzadeh S, Srivastava SC (1992) Improved specific activity of reactor produced <sup>117m</sup>Sn with the Szilard-Chalmers process. *Int J Appl Radiat Isot* 43:1117–1122
- Mausner LF, Kolsky KL, Mease RC et al (1993) Production and evaluation of Sc-47 for radioimmunotherapy. *J Labelled Comp Radiopharm* 32:388–390
- Mausner LF, Kolsky KL, Joshi V, Sweet MP, Meinken GE, Srivastava SC (2000) Scandium 47: a replacement for Cu-67 in nuclear medicine therapy with beta/gamma emitters. In: Stevenson N (ed) *Isotope production and applications in the twenty first Century*, 2000. World scientific, London, pp 43–45
- McDevitt MR, Finn RD, Sgouros G (1999) An Ac-225/Bi-213 generator system for therapeutic clinical applications: construction and operation. *Appl Radiat Isot* 50:895
- Mease RC, Mausner LF, Srivastava SC (1997) Macrocyclic polyaminocarboxylates for radiometal antibody conjugates for therapy, SPECT and PET imaging. US Patent #5,639,879, June 17, 1997
- Medvedev D, Mausner LF, Srivastava SC (2011) Irradiation of strontium chloride targets at proton energies above 35 MeV to produce PET radioisotope Y-86. *Radiochim Acta* 99:755–761
- Medvedev DJ, Mausner LF, Meinken GE et al (2012) Development of large scale production of Cu-67 from Zn-68 at the high energy accelerator: closing the Zn-68 cycle. *Int J Appl Radiat Isot* 70:423–429
- Meinken GE, Kurczak S, Mausner LF, Kolsky KL, Srivastava SC (2005) Production of high specific activity Ge-68 at Brookhaven National Laboratory. *J Radioanal Nucl Chemistry* 263:553–557
- Melville G, Allen BJ (2009) Cyclotron and linac production of Ac-225. *Appl Radiat Isot* 67(4):549–555
- Miederer M, Henriksen G, Alke A et al (2008a) Preclinical evaluation of the alpha-particle generator nuclide Ac-225 for somatostatin receptor radiotherapy of neuroendocrine tumors. *Clin Cancer Res* 14:3555
- Miederer M, Scheinberg DA, McDevitt MR et al (2008) Realizing the potential of the actinium-225 radionuclide generator in targeted alpha particle therapy applications. *Adv Drug Deliver Rev* 60:1371
- Mikheev V, Popvich VB, Rumer IA, Savelev GI, Volkova NC (1972) Re-188 generator. *Isotopenpraxis* 8:248–250
- Mirzadeh S, Walsh P (1998) Numerical evaluation of the production of radionuclides in a nuclear reactor, Part I&II. *Appl Radiat Isot* 49:370–383
- Mirzadeh S, Parekh PP, Katcoff S, Chu YY (1983) Cross-section systematics for nuclide production at a medium energy spallation neutron facility. *Nucl Instrum Methods* 216:149–154
- Mirzadeh S, Mausner LF, Srivastava SC (1986) Production of no-carrier-added Cu-67. *Int J Radiat Appl Instrum Part A, Appl Radiat Isot* 37:29–36
- Mirzadeh S, Knapp FF Jr, Lambrecht RM (1997a) Burn-up cross-section of W-188. *Radiochim Acta* 77:99–102
- Mirzadeh S, Knapp FF Jr, Alexander CW, Mausner LF (1997b) Evaluation of neutron inelastic scattering for radioisotope production. *Appl Radiat Isot* 48:441–446
- Mirzadeh S, Du M, Beets AL, Knapp FF Jr (2000) Thermoseparation of neutron irradiated tungsten from Re and Os. *Ind Eng Chem Res* 39:3169–3172
- Mughabgab SF, Divadeenam M, Holden NE (1984) *Neutron cross-sections*. Academic Press, New York
- Narula J, Srivastava S, Petrov A et al (2012) Evaluation of tin-117m labeled Annexin V for imaging atherosclerotic lesions in a hyperlipidemic rabbit model. Publication in progress

- Neves M, Kling A, Olivera A (2005) Radionuclides used for therapy and suggestion for new candidates. *J Radioanal Nucl Chem* 266:377–384
- Norenberg JP, Krenning BJ, Konings I et al (2006) Bi-213-DOTA(0),Tyr(3) octreotide peptide receptor radionuclide therapy of pancreatic tumors in a preclinical animal model. *Clin Cancer Res* 12:897
- O'Donoghue JA, Bardies M, Wheldon TE (1995) Relationships between tumor size and curability for uniformly targeted therapy with beta emitting radionuclides. *J Nucl Med* 36:1902–1909
- Oster ZH, Som P, Srivastava SC et al (1985) The development and in-vivo behavior of tin containing radiopharmaceuticals II: Autoradiographic and scintigraphic studies in normal animals and in animal models of bone disease. *Int J Nucl Med Biol* 12:175–184
- Qaim SM, Döhler H (1984) Production of carrier-free  $^{117m}\text{Sn}$ . *Int J Appl Radiat Isot* 35:645–650
- Qaim SM, Stocklin G (1983) Production of some medically important short-lived neutron deficient radioisotopes of halogens. *Radiochim Acta* 34:25–40
- Richards P, Tucker WD, Srivastava SC (1982) Technetium-99m: an historical perspective. *Int J Appl Radiat Isot* 33:793
- Sadeghi M, Aboudzadeha M, Zali A et al (2009) Radiochemical studies relevant to Y-86 production via  $^{86}\text{Sr}(p, n)^{86}\text{Y}$  for PET imaging. *Appl Radiat Isot* 67:7–10
- Scheinberg DA, Strand MA (1983) Kinetic and catabolic considerations of monoclonal antibody targeting in erythroleukemia mice. *Cancer Res* 43:265–272
- Schlyer DJ (2003) Production of radionuclides in accelerators. In: Welch MJ, Redvanly CS (eds) *Handbook of radiopharmaceuticals*, Wiley, Chichester
- Smith SV, Di Bartolo N, Mirzadeh S, Lambrecht RM, Knapp FF Jr (1995) [ $^{166}\text{Dy}$ ] Dysprosium/[ $^{166}\text{Ho}$ ] holmium in vivo generator. *Appl Radiat Isot* 46:759–764
- Sofou S, Kappel BJ, Jaggi JS et al (2007) Enhanced retention of the alpha-particle-emitting daughters of actinium-225 by liposome carriers. *Bioconj Chem* 18:2061
- Srivastava SC (ed) (1988) *Radiolabeled monoclonal antibodies for imaging and therapy*. Plenum Press, New York, p 876
- Srivastava SC (1996a) Therapeutic radionuclides: making the right choice. In: Mather SJ (ed) *Current directions in radiopharmaceutical research and development*, Kluwer Academic Publishers, Dordrecht, pp 63–79
- Srivastava SC (1996b) Criteria for the selection of radionuclides for targeting nuclear antigens for cancer radioimmunotherapy. *Cancer Biother Radiopharm* 11:43–50
- Srivastava SC (1996c) Is there life after technetium: what is the potential of developing new broad-based radionuclides. *Semin Nucl Med* 26:119–131
- Srivastava SC (2006) Radionuclide therapy with high-LET electron emitters: therapeutic applications of conversion electron emitter tin-117m. In: Mazzi U, Eckelman WC, Volkert WA et al (eds) *Technetium, rhenium, and other metals in chemistry and nuclear medicine*. SG Editoriali, Padova, pp 553–568
- Srivastava SC (2009) “Theragnostic” radiopharmaceuticals: the ‘Janus’ approach to molecular diagnosis and therapy. CME session # 63 on novel radiopharmaceuticals for molecular imaging and therapy—where are we headed next? Presented at 2009 SNM annual meeting, Toronto, Canada, June 15, 2009
- Srivastava SC (2010) Theragnostic radiometals: getting closer to personalized medicine. In: Mazzi U et al (eds) *Technetium and other radiometals in chemistry and nuclear medicine 2010*, SG Editoriali, Padova, pp 553–568
- Srivastava SC (2011) Paving the way to personalized medicine: production of some theragnostic radionuclides at Brookhaven National Laboratory. *Radiochim Acta* 99:635–640
- Srivastava SC (2012) Paving the way to personalized medicine: production of some promising theragnostic radionuclides at Brookhaven National Laboratory. *Semin Nucl Med* 42:151–163
- Srivastava SC, Dadachova E (2001) Recent advances in radionuclide therapy. *Semin Nucl Med* 31:330–341
- Srivastava SC, Mease RC (1991) Progress in research on ligands, nuclides, and techniques for labeling monoclonal antibodies. *Nucl Med Biol* 18:589–603
- Srivastava SC, Atkins HL, Krishnamurthy GT et al (1998) Treatment of metastatic bone pain with tin-117m(4+)DTPA: a phase II clinical study. *Clinical Cancer Res* 4:61–68
- Srivastava SC, Toporov YuG, Karelin EA, Vakheto FZ, Andreev OI, Tselishev IV, Popov YuS (2004) Reactor production of high-specific activity tin-117m for bone pain palliation and bone cancer therapy. *J Nucl Med* 45:475P
- Srivastava SC, Gonzales G, Narula J, Strauss HW et al (2012a) Development and evaluation of tin-117m labeled Annexin for the imaging and treatment of vulnerable plaques. Publication in Progress
- Srivastava SC, Gonzales G, Adzic R, Meinken GE (2012b) Method of electroplating a conversion electron emitting source on implant. US Patent Application Serial No. 11/758,914, Dec 22, 2011; Publication in progress
- Swailem FM, Krishnamurthy GT, Srivastava SC et al (1998) In-vivo tissue uptake and retention of Sn-117m (4+) DTPA in a human subject with metastatic bone pain and in normal mice. *Nucl Med Biol* 25:279–287
- Sweet MP, Mease RC, Srivastava SC (2000) Rigid bifunctional chelating agents. US Patent # 6,022,522, Feb 8, 2000
- Szelecsenyi F, Blessing G, Qaim SM (1993) Excitation functions of proton induced nuclear reactions on enriched  $^{61}\text{Ni}$  and  $^{64}\text{Ni}$ : possibility of production of no-carrier-added  $^{61}\text{Cu}$  and  $^{64}\text{Cu}$  at a small cyclotron. *Appl Radiat Isotopes* 44:575–580
- Traub-Weidinger T, Raderer M, Uffman M et al (2011) Improved quality of life in patients treated with peptide radionuclides. *World J Nucl Med* 10:115–121
- Volkert WA, Goeckler WF, Ehrhardt GJ et al (1991) Therapeutic radionuclides: production and decay property considerations. *J Nucl Med* 32:174–185
- Weber DA, Eckerman KF, Dillman LT, Ryman JC (1989) *MIRD: radionuclide data and decay schemes*, Society of Nuclear Medicine, New York
- Weinreich R (ed) (1992) *Targetry '91*. Proceeding of the IVth international workshop in targetry and target chemistry. Paul Scherrer Institute 92-01, Villigen, Switzerland
- Wessels BW, Rogus RD (1984) Radionuclide selection and model absorbed dose calculations for radiolabeled tumor-associated antibodies. *Med Phys* 11:638–645
- Wessels BW, Griffith MH, Bradley EW et al (1985) Dosimetric measurements and radiobiological consequences of radioimmunotherapy in mice. In: Schlafek-Stelson AT, Watson EE (eds) *Fourth international radiopharmaceutical dosimetry*. Oak Ridge Associated Universities, Oak Ridge, pp 446–457
- Wheldon TE, O'Donoghue JA (1990) The radiobiology of targeted radiotherapy. *Int J Radiat Biol* 58:1–21
- Wilbur DS (1990) Potential use of alpha emitting radionuclides in the treatment of cancer. *Antib Immunoconj Radiopharm* 4:85–97
- Yamazaki T, Ewan GT (1969) Level and isomer systematics in even tin isotopes from Sn-108 to Sn-118 observed in Cd( $\alpha$ , xn) Sn reactions. *Nucl Phys A* 134:81–109
- Yao Z, Garmestani K, Wong KJ et al (2001) *J Nucl Med* 42:1538–1544

- Yorke ED, Beaumier PL, Wessels BW (1991) Optimal radionuclide-antibody combinations for clinical radioimmunotherapy: A predictive model based on mouse pharmacokinetics. *Nucl Med Biol* 18:827–835
- Zalutsky MR, Zhai X-C, Alston KL (2001) High level production of alpha-particle emitting At-211-labeled antibodies for clinical use. *J Nucl Med* 42:1508–1515
- Zhuikov BL, Kalmykov SN, Ermolaev SV et al (2011) Production of  $^{225}\text{Ac}$  and  $^{223}\text{Ra}$  by irradiation of Th with accelerated protons. *Radiochemistry* 53:73–80
- Zhuikov B, Srivastava SC, Ermolaev SV et al (2012) Production of no-carrier-added Sn-117m at medium energy cyclotrons. Publication in progress



<http://www.springer.com/978-3-540-36718-5>

Therapeutic Nuclear Medicine

Baum, R.P. (Ed.)

2014, XVIII, 951 p. 600 illus., 300 illus. in color.,

Hardcover

ISBN: 978-3-540-36718-5